*Ecology*, 92(8), 2011, pp. 1648–1657


# Inferring ecological and behavioral drivers of African elephant movement using a linear filtering approach

Alistair N. Boettiger,[1] George Wittemyer,[2,3,7] Richard Starfield,[4] Fritz Volrath,[3,5] Iain Douglas-Hamilton,[3,5] and Wayne M. Getz[4,6]

[1]*Biophysics Graduate Program, University of California, Berkeley, California 94720-3112 USA*
[2]*Department of Fish, Wildlife and Conservation Biology, Colorado State University, 1474 Campus Delivery, Fort Collins, Colorado 80523 USA*
[3]*Save the Elephants, P.O. Box 54667, Nairobi 00200 Kenya*
[4]*Department of Environmental Science, Policy, and Management, University of California, 137 Mulford Hall, Berkeley, California 94720-3112 USA*
[5]*Oxford University, Department of Zoology, Oxford OX1 3PS United Kingdom*
[6]*Mammal Research Institute, University of Pretoria, Pretoria 0001 South Africa*

*Abstract*. Understanding the environmental factors influencing animal movements is fundamental to theoretical and applied research in the field of movement ecology. Studies relating fine-scale movement paths to spatiotemporally structured landscape data, such as vegetation productivity or human activity, are particularly lacking despite the obvious importance of such information to understanding drivers of animal movement. In part, this may be because few approaches provide the sophistication to characterize the complexity of movement behavior and relate it to diverse, varying environmental stimuli. We overcame this hurdle by applying, for the first time to an ecological question, a finite impulse–response signal-filtering approach to identify human and natural environmental drivers of movements of 13 free-ranging African elephants (*Loxodonta africana*) from distinct social groups collected over seven years. A minimum mean-square error (MMSE) estimation criterion allowed comparison of the predictive power of landscape and ecological model inputs. We showed that a filter combining vegetation dynamics, human and physical landscape features, and previous movement outperformed simpler filter structures, indicating the importance of both dynamic and static landscape features, as well as habit, on movement decisions taken by elephants. Elephant responses to vegetation productivity indices were not uniform in time or space, indicating that elephant foraging strategies are more complex than simply gravitation toward areas of high productivity. Predictions were most frequently inaccurate outside protected area boundaries near human settlements, suggesting that human activity disrupts typical elephant movement behavior. Successful management strategies at the human–elephant interface, therefore, are likely to be context specific and dynamic. Signal processing provides a promising approach for elucidating environmental factors that drive animal movements over large time and spatial scales.

*Key words: African elephant; landscape dynamics;* Loxodonta africana; *movement ecology; NDVI; prediction; radio-tracking; signal processing; spatiotemporal landscape; Weiner filter*.

## Introduction

Linking movements of animals to underlying landscape features is critical to identify factors motivating animal spatial behavior (Lima and Zollner 1996) and resulting population spatial distributions (Turchin 1991, Johnson et al. 1992). However, traditional approaches, such as the well-established framework of Lagrangian random walk and Eulerian diffusion processes, are typically applied on either featureless or minimally structured landscapes (Kareiva and Shigesada 1983, Bergman et al. 2000, Edwards et al. 2007, Bartumeus et al. 2008). Beyond simply relating movement to landscape characteristics, current research calls attention to the importance of relating movement to temporal and spatial dynamics of landscape features (Bowler and Benton 2005, Mueller and Fagan 2008).

Understanding the relationship between landscape dynamics and movement is particularly important to wide-ranging species whose mobility can be critical for persistence in the face of high temporal variability of local food resources (Fryxell et al. 2005, 2008, Hebblewhite et al. 2008). Generally, foraging resources are recognized as a predominant factor influencing movement (Berger 2004), which for herbivores is increasingly investigated using spatially and temporally specific vegetation productivity indices (e.g., normalized difference vegetation index, NDVI; see Fryxell et al. 2005,

Manuscript received 18 January 2010; revised 8 October 2010; accepted 4 February 2011; final version received 5 March 2011. Corresponding Editor: B. P. Kotler.

[7] Corresponding Author. E-mail: g.wittemyer@colostate.edu

Pettorelli et al. 2005, Hebblewhite et al. 2008, Mueller and Fagan 2008). In addition to dynamics in forage availability and quality, other landscape features may shape movement and population distributions. Numerous welfare factors are critical to animal population persistence and strongly shape distributions (Simpson et al. 2006, Holdo et al. 2009). At the same time, human activity is increasingly a dominant feature of most ecosystems (Sanderson et al. 2002), with roads frequently being identified as major barriers to animal movement (Forman and Alexander 1998). Assessing the influence of the variety of ecosystem components encountered by mobile species is critical to gaining holistic understanding of the determinants of animal movement and resulting population distributions.

In this study, we explore the importance of multiple static and dynamic landscape features for predicting movement of free-ranging African elephants (*Loxodonta africana*). African elephants range widely and can exhibit multiple movement strategies within the same ecosystem (Wittemyer et al. 2007*a*, 2008). Habitat fragmentation and human incursions into historic rangelands is a critical conservation issue impacting the species across its range (Blanc et al. 2007). Yet little analysis of the diversity of potential factors influencing elephant movement strategies has been conducted (but see Loarie et al. 2009). Here we investigate movement paths collected over a seven-year period for 13 wild African elephants that were the principal members of social groups ranging in size from six to 19 individuals. We use the ~0.5 million GPS positions that characterize the movement tracks to study the influence of landscape covariates including spatiotemporally dynamic NDVI and proximity to static landscape features of water, roads, and park boundaries.

Recent analytical advances that incorporate landscape features directly in models of animal movement are being applied more frequently (Preisler et al. 2004, Dalziel et al. 2008, Getz and Saltz 2008, Patterson et al. 2008, Schick et al. 2008), though accounting for dynamics at a fine scale is still relatively rare. Here we introduce a novel approach using a signal-filtering framework that allows study of the relationship between animal movement and ecological landscape dynamics. The approach is based on easy-to-interpret linear correlations among model inputs, a construction similar to movement path reconstruction using a Kalman filter (Sibert et al. 2003, Lam et al. 2008, Royer and Lutcavage 2008). Rather than focusing on error correction, we construct a linear time series model that predicts future movement pathways from a finite set of past movement data and current values of pertinent landscape covariates by minimizing the mean square error (MSE) between the predicted (i.e., filtered) second-order data statistics and observed second-order statistics (Hayes 1996). Such models (also known as finite impulse response Wiener filters) assess the relative importance of past movement patterns and landscape covariates to determine future movement pathways by quantifying the strength of different signal components for movement pattern prediction.

Application of linear filtering to movement data, as presented here, tackles several fundamental questions in the field of movement ecology (Patterson et al. 2008). (1) To what extent do models that account for landscape factors outperform simpler correlated random walk (CRW) models, whether Gaussian or Lévy (Edwards et al. 2007)? (2) What factors on the landscape influence the movement of individuals at localized times and points in space and how are they functionally related? (3) How differentiated are individual movement responses to landscape characteristics? (4) What new information is gained through predictive modeling of movement that serves wildlife and biodiversity management and conservation goals?

## Methods

### *Study site*

Our analyses focus on the movements of elephants inhabiting the Samburu and Buffalo Springs National Reserves in northern Kenya. This semiarid region is dominated by *Acacia–Commiphora* savanna and scrub bush and the reserves are focused on the major permanent water source in the region, the Ewaso N'giro River (Barkham and Rainy 1976). Over the past 40 years, rainfall has averaged ~350 mm/yr, with the majority falling during biannual rainy seasons generally taking place in April and November (G. Wittemyer, *unpublished data*). The reserves are not fenced and the study elephants are free-ranging, moving in and out of the reserves year round (Douglas-Hamilton et al. 2005, Wittemyer et al. 2007*a*). Thus the movement paths analyzed here are not restricted by fences or impassible geographic barriers. The 13 elephants tracked represent 13 distinct social groups ranging in size from 6 to 19 individuals, and represent >25% of the resident elephants using the study area (Wittemyer et al. 2009*b*). Separate analysis demonstrated that group members are consistently in direct proximity (Wittemyer et al. 2009*b*); therefore the movements of the tracked individuals are assumed to represent the group's movements.

### *Movement data*

Elephant movements were tracked using global positioning system (GPS) collars, which collected GPS positions at 15-min, 1-h, or 3-h time intervals (the latter to conserve power during the last few weeks of a collar's life). GPS failures, low sampling resolution during power-saving modes, and erroneous fixes accounted for <10% of expected hourly positions. Accuracy of locations from GPS tracking data is typically within 5–20 m, representing <5% of the distance covered during average hourly movements.

To obtain a measure of daily location, thereby ameliorating differences in GPS sampling frequency

and failures, we used the smallest ellipse that contained all GPS points over the previous 24 h. These ellipses are characterized by the longitude and latitude of the centroid or center of motion (CoM), the lengths of the major and minor axes, and the orientation (direction of major axis: see Appendix: Fig. A1). For computational efficiency, we omitted fitting the least informative parameter: the minor axis. Because our analysis emphasizes the average daily quality of behavior rather than individual hour-to-hour movements, it is useful for detecting seasonal or landscape factors that affect the extent or direction of daily movements.

### *Data on landscape features*

The underlying landscape features that we assessed as drivers of movement behavior (question 2) were: digitized locations of static features (protected area boundaries, permanent watercourses, and major roads converted to "distance from feature" raster maps at a resolution of ~550 m or 0.005°); NASA digital elevation data (Shuttle Radar Topographic Mission) at a spatial resolution of 90 m (<0.001°); 10-day (three times per month) composite time-specific NDVI values (Satellite Probatoire d'Observation de la Terre systems); and a location-specific seasonal index inferred from average regional NDVI (Wittemyer et al. 2007*b*). In the model, time-specific NDVI averages were computed over a 1-km circle centered on the CoM location, and NDVI averages over eight directional segments filling the area between this inner 1 km and an outer 6-km circle were computed (Appendix: Fig. A2).

In summary, the elephant movement data were assumed to depend on the following 17-dimensional landscape feature vector: (1) CoM latitude, (2) CoM longitude, (3) length of long ellipse axis, (4) orientation of ellipse axis, (5–13) one inner and eight outer NDVI sectors, (14) distance to permanent water, (15) distance to roads, (16) distance to protected area boundary, and (17) ecosystem average NDVI (seasonal signal). Because tracking data were not continuous for any single elephant over the seven-year study, all time-dependent data (NDVI or season) were collated to match each elephant's GPS data such that sections lacking position data were excluded from these other time series data. Finally, before any filtering, all data were normalized to a common interval, [−1,1]. This was necessary to facilitate the subsequent analysis of the filter structure and comparison across individuals (question 3).

### *Signal-processing framework*

Signal processing is a well-established data analysis tool focusing on the predictive performance of model input variables (Hayes 1996). We recorded the values of the 17 signal inputs, represented by $\mathbf{s}[n]$, where the square brackets indicate that the vector is sampled in discrete time, in this case 500 hourly intervals indexed by $n$; $n$ is always a variable, so $f[n]$ is a function of time, where $f[n = k]$ is the single scalar value that the function $f$ takes when evaluated at $n = k$. We selected 500 h (4 h short of 3 weeks) for reasons elaborated in the Appendix (*Insights from model structure* and Appendix: Fig. A3). The approach also requires that we select a parameter $p$ that is the number of consecutive time points from the signal $\mathbf{s}[n]$ (i.e., $\mathbf{s}[n = k]$, $\mathbf{s}[n = k - 1]$, . . . , $\mathbf{s}[n = k - p + 1]$) to predict a vector $\mathbf{d}[n = k + 500]$ 500 h later. In our case, $\mathbf{d}[n]$ is a four-dimensional characterization (CoM longitude, CoM latitude, length of major axis, and orientation of major axis) of the smallest ellipse that contains all the movement data for the 24-h period starting at time $n$. Mathematically, $\mathbf{d}^*[n = k]$ is an estimate of $\mathbf{d}[n = k + 500]$ (i.e., we use the superscript asterisk to emphasize that we use data at time $k - p + 1, \ldots, k$, to predict data at time $k + 500$) computed from $\mathbf{s}[n]$ by convolving $\mathbf{s}[n]$ with a finite impulse response filter, $\mathbf{W}[n]$:

$$d_j^*[n] = \sum_{i=1}^{N} \sum_{k=0}^{p-1} s_i[n - k] W_{i,j}[k] \qquad (1)$$

where $j = 1, \ldots, 4$ indexes the different elements of $\mathbf{d}^*[n]$; $i = 1, \ldots, N$ indexes the different elements of $\mathbf{s}[n]$; and the sum over $k$ performs the time convolution of the signal component $s_i$ with the appropriate component of the filter $\mathbf{W}[n]$. We write $i$ going up to $N$ because, in general, we may use a variable number of signals in order to make our predictions (e.g., to see if anything is lost by excluding a given signal). The filter $\mathbf{W}[n]$ is determined from the second-order statistics of $\mathbf{s}[n]$ and $\mathbf{d}[n]$, chosen to minimize the squared difference between the prediction, $\mathbf{d}^*[n = k]$, and the actual future, $\mathbf{d}[n = k + 500]$. This calculation of filter coefficients from statistical properties > of the signal and the data is a standard method in stochastic signaling processing and is described in detail in the Appendix. It assumes that the autocorrelation and cross-correlation do not change during the 500-h sampling interval, and that the output data depend only on the difference in time between when the signal is measured and the time for which a prediction will be made.

Due to both computational constraints and to avoid over-fitting filter coefficients, it is desirable to keep $p$ as small as possible. It is important, however, not to overly constrain the model to an arbitrarily recent past if longer timescale correlations are a driving component in the underlying system. A systematic exploration of our data indicated that $p = 5$ (i.e., using the last five hours of movement data) was sufficient for reasonable prediction. For this choice of $p$, the dimensionality of the filter is still two orders of magnitude smaller than the dimension of the data, and prediction accuracy is similar to that achieved with higher dimensional filters. All results presented in the text use this value. Thus, in summary, we use five consecutive hourly points of movement (i.e., the movement ellipse) and landscape data contained in the 17-dimensional vector $\mathbf{s}[n]$ at times $n = k - 4, \ldots, k$ to predict the four-dimensional movement data vector $\mathbf{d}[n]$ alone at time $n = k + 500$, where the movement data vector is the smallest ellipse that contains the actual

TABLE 1. Median and interquartile ranges (IQR) of normalized mean-square error (MSE) of predicted African elephant movements from filters fitted to different combinations of input data, with associated input dimensions.

| Input data | MSE of predicted $\mathbf{d}[n]$ | | Input dimension | MSE of predicted CoM (km) | |
|---|---|---|---|---|---|
| | Median | IQR | | Median | IQR |
| All | 0.12 | (0.12, 0.13) | 17 | 1.21 | (0.88, 1.43) |
| Previous movement | 0.24 | (0.20, 0.25) | 4 | 2.20 | (1.76, 2.97) |
| CoM | 0.41 | (0.36, 0.64) | 2 | 2.64 | (2.09, 3.74) |
| NDVI | 0.23 | (0.21, 0.27) | 9 | 1.87 | (1.54, 2.75) |
| Static features | 0.23 | (0.21, 0.28) | 3 | 2.42 | (2.20, 2.64) |
| Human | 0.27 | (0.22, 0.34) | 2 | 2.42 | (2.09, 3.30) |
| Water | 0.40 | (0.33, 0.61) | 1 | 2.75 | (2.20, 4.18) |
| Null model | 3.40 | (2.84, 4.91) | 2 | NA | |

*Notes:* Translation of normalized error to average error (in km) focusing exclusively on the center of mass (CoM) movement output is presented. The best movement prediction (lowest MSE) was derived from the combination of all inputs. Predictions using any signal input or combination of signal inputs exceeded those from the correlated random walk null model. NDVI is the normalized difference vegetation index. The vector $\mathbf{d}[n]$ is a unitless, four-dimensional characterization (CoM longitude, CoM latitude, length of major axis, and orientation of major axis) of the smallest ellipse that contains all the movement data for the 24-h period starting at time $n$; square brackets indicate that the vector is sampled in discrete time.

position point data of that individual for the 24-h period starting at time $n = k$. Therefore, we are predicting the general location of the individual over a 24-h period of time, not the actual GPS location on the landscape at a specific hour.

### *Error calculation*

Signal statistics are computed empirically from the data in order to solve for the filter $\mathbf{W}[k]$ in Eq. 1. The time histories of the 17 signal input parameters over 500 h were fed into the filter to predict the complete trajectory of movement ellipses for the subsequent 500 h. Performance was assessed by taking the mean of the squared difference between the recorded movement ellipses and the predicted ellipses. Information regarding further error normalization is provided in the Appendix.

### *Null model comparison and filter performance analyses*

The performances of filters using various signal inputs and applied across time and elephants were compared with that of a correlated random walk (CRW) model (addressing question 1): i.e., a stochastic process that had the same "distance moved" and correlated direction of heading statistics as the time-specific data being fitted, but without reference to landscape data or past position. Specifically, $\mathbf{x}[n] = \mathbf{A}\mathbf{x}[n - 1] + \mathbf{w}$, where $\mathbf{x}$ is the two-dimensional displacement vector, $\mathbf{w}$ is a two-dimensional white Guassian random number (with $x$ and $y$ variance chosen to match the behavior of the elephant being represented), and $\mathbf{A}$ is a diagonal matrix containing the $x$ and $y$ correlation coefficients for displacement. The MSE performance of this CRW model provided the baseline against which the MSE estimates (a measure of the predictive capabilities) of the various filters were compared.

The MSE performances of the CRW null model were also compared to the MSE performances of (1) filters applied to noncontiguous sections of data from the same elephant (e.g., filter fitted to movements from April applied to predict movements in November), an objective associated with question 2; and (2) filters applied across different elephants (e.g., filters fitted to the movement of one elephant applied to predict the movement of another elephant), an objective associated with question 3. For predictive performance comparison of filters fitted to statistics of a particular period and applied to predict movements at noncontiguous periods, application was restricted in the following manner in order to investigate underlying properties influencing predictive performance: (1) no restrictions: any noncontiguous data; (2) time $< 3$: data within 3 months of the original data; (3) time $> 3$: data beyond 3 months of the original data; (4) similar season: during seasonally similar periods (defined from ecosystem average NDVI as periods when average NDVI was within 0.2 of the normalized range of values during the time when the filter was fitted), and (5) nearby: data within a normalized distance of 0.2 of the original location of data (see Appendix for details). In addition, MSE for filter application across all possible combinations of these restrictive categories was assessed. Direct analysis of the possible relationship between landscape context and filter performance was assessed by mapping the locations of high prediction error (see Appendix for details).

## RESULTS

### *Predictive performance of different Weiner filters*

As a fundamental assessment of the efficacy of the Weiner filter approach, we compared the predictive power of a correlated random walk (CRW) model (lacking any information on landscape context) to that of Weiner filters with different signal inputs, thereby addressing question 1 posited in the *Introduction*. Regardless of signal input structure, the predictive power of Weiner filters had median MSE fits that, on average (across 13 elephants with fits in different seasons and years), were more than an order of magnitude smaller than fits of the CRW null model (Table 1).

Over large sections of the data set, our Weiner filter provided credible predictions of actual 24-h movement behaviors by filtering the signal variables from the previous three weeks (Fig. 1). MSE estimates resulting

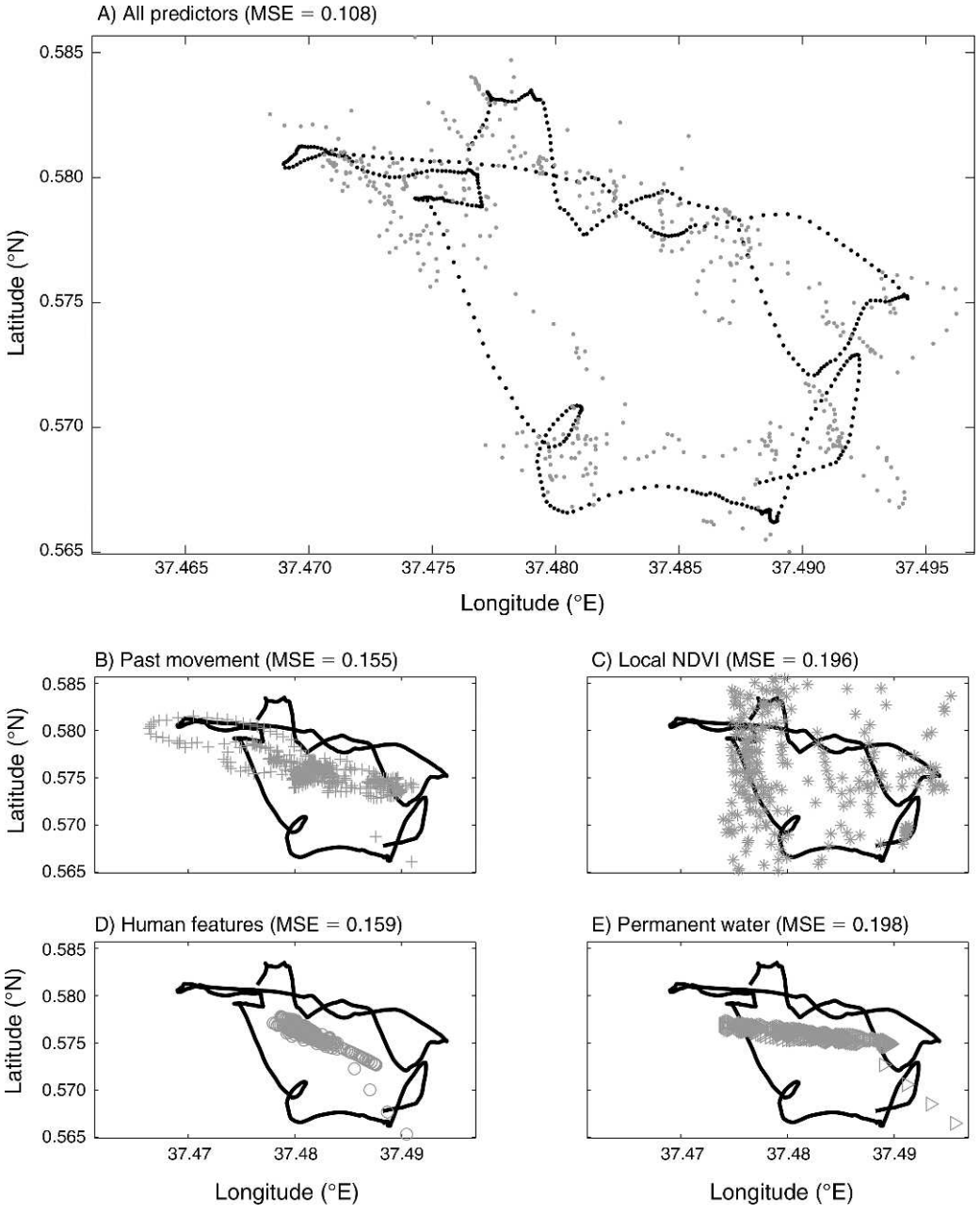


FIG. 1. Predicted vs. real movement patterns of African elephants, based on different signal data. (A) Predicted movement paths of African elephants derived from linear Weiner filters (gray dots: 500 sequential hours of CoM [center of motion; see *Methods*] produced by filters fitted to the preceding 500-h actual movement path and landscape data segments) were generally similar to actual movement paths (black dots) during the predicted period when all signal inputs were used in filter construction. In the lower panels (gray, predicted paths; black, actual paths), filters that predicted movement contained a subsection of the signal inputs: (B) past movement only; (C) NDVI (normalized difference vegetation index) only; (D) anthropogenic landscape features only; and (E) permanent water only. Mean-square error estimates (MSE) for the predicted movement paths (above each panel) are similar to median values reported in Table 1, allowing visualization of approximate performance.

from the full Weiner filter were similar across elephants (Appendix: Table A1); this indicated that, on average, differences in home range size and extent of tracking data did not affect predictive performance. In order to calculate actual spatial accuracy of predictions, a parallel analysis was conducted focusing exclusively on non-normalized CoM estimation to allow calculation of MSE in spatial units. Results showed that typical predictions were off by ~0.88–1.43 km or ~20% of a daily movement (Table 1). However, it is important to note that predicting movement behavior from CoM alone performs significantly worse than when using all

four movement ellipse parameters (Wilcoxon rank sum: $Z = 4.3$, $n = 13$, $P < 0.001$).

To address question 2 and evaluate the influence of landscape features (i.e., filter signal inputs) on movement prediction, MSE estimates of predictions made using different filters were assessed independently and compared (Fig. 2). The relative performance of the three classes of signal inputs, previous movements (i.e., relying on autocorrelation signatures in movements), static landscape features (permanent rivers, major roads, and park boundaries), or NDVI provided similar predictive performance (i.e., MSE values across inputs were not significantly different) when averaged over time (Appendix: Table A1); median results are presented in Table 1. For any given set of predictions, however, the MSE can vary considerably among these three signals (see Appendix: Fig. A4), with periods when NDVI, past movement, or landscape features are the predominant correlate of movements and other periods when these features do not independently exert any measurable influence on movement behavior.

Predictive performance increased as multiple inputs were combined, indicating that elephants react to a combination of multiple sources of information on landscape characteristics. For instance, performance of the static landscape features decreased when human-created landscape features (protected area boundaries and major roads) and natural features (distance from permanent water) were separated (Table 1). Also predictive performance based on NDVI was not simply a function of elephants moving to areas of higher NDVI (Appendix: Fig. A5). In contrast to expectations and results derived from different methods (Loarie et al. 2009), no significant differences were found in the propensity to move to local locations with higher, rather than lower, NDVI (Wilcoxon signed-rank test: $W = 1$, $n = 13$, $P = 0.954$).

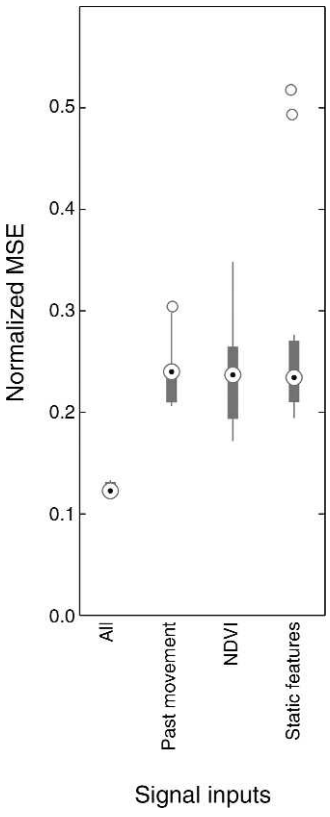


FIG. 2. The best movement prediction (significantly lower MSE) was derived from the combination of all signal inputs (all factors) as shown by median and interquartile range (IQR, 25th and 75th percentile) of the median MSE filter performance of the 13 elephants studied. Individual signal components of previous movement, vegetation productivity (NDVI), and static landscape features (roads, protected area [PA] boundaries, and permanent water) did not differ significantly. Predictions using any signal input or combination of signal inputs exceeded those from the null model (Table 1: MSE = 3.4) by an order of magnitude. Outliers are defined as points that lie two times the distance between the third and first quartiles beyond the quartile boundaries (gray box; dots indicate the median MSE), and whiskers extend to the farthest point not considered an outlier.

### *Applying filters across time, seasons, locations, and elephants*

To test the general applicability of filter structure across time (addressing aspects of question 2), filters fitted to statistics of a particular period were applied to predict movements at all other noncontiguous periods in an elephant's data set (i.e., unmatched filters). Such analysis provides a measure of the degree to which patterns captured by a given filter are temporally specific. Noncontiguous filters performed significantly worse than contiguous filters, with an order of magnitude greater MSE (Fig. 3: see Appendix: Fig A6 and Table A2). Noncontiguous filter performance (MSE = 2.78; Appendix: Table A2) was slightly, but not significantly, better than that of the null CRW model (MSE = 3.51; Table 1); it should be noted that equitable comparison is difficult, given that the null model performance is calculated for statistics from data of contiguous periods rather than across noncontiguous periods.

To address question 3, filters fitted to one elephant were used to predict the movements of each other elephant. MSE values of filters applied across different elephants were significantly greater than MSE of noncontiguous filters fitted to the parent elephant (Wilcoxon signed-rank test: $W = 91$, $n = 13$, $P = 0.0016$; Fig. 3). This suggests that there are elephant-specific response behaviors captured by each filter. If we restricted comparisons to the same season (conditions within 20% of the seasonal NDVI signals during origination), the same approximate time (applying the filter to data occurring within 3 months), or a similar location (i.e., "nearby" defined as within 20% of the elephant's range) improvement in performance resulted. Across such constraints, prediction error was consistently lowest for filters applied to data from the parent elephant (in contrast to a different elephant; Fig. 3), indicating that elephant-specific behaviors captured by the filter are not purely due to similarities in range or

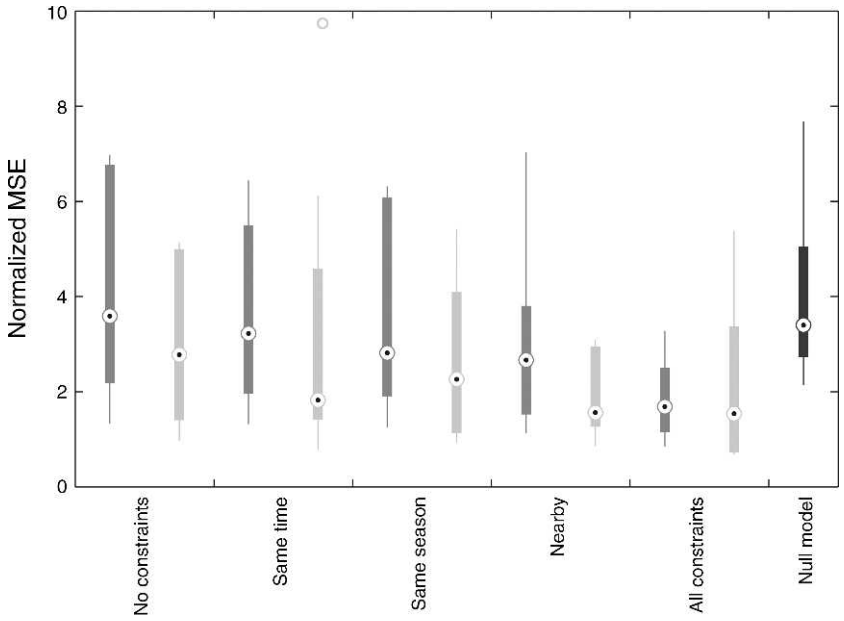


FIG. 3. Noncontiguous filter performance (portrayed as median and IQR of per elephant median MSE performance) increased when application of the filter was restricted to predict data that were temporally similar (i.e., within 3 months; $t$), from the same season, and near the location of the original data, with a combination of these three restrictions ("all constraints") resulting in the best fit. Application of filters fit to noncontiguous data from the same elephants (light gray) outperformed those applied across elephants (i.e., filter fit to the movements of one elephant used to predict the movements of another elephant; dark gray), regardless of restrictions. The performance of noncontiguous predictions without restrictions was not significantly different from that of the null model (Wilcoxon signed-rank test: $W = 25$, $n = 13$, $P = 0.390$), although performance when restricted in time, season, and position was significantly better than that of the null ($W = 61$, $n = 13$, $P = 0.035$). Outliers and whiskers are as defined for Fig. 2.

temporal overlap. Simultaneous constraint of location, season, and time resulted in the greatest reduction.

### *Spatial analysis of errors*

Small intervals in which filter predictions were completely inconsistent with actual movements occurred infrequently. The locations of individuals during such "high error" intervals, however, were not randomly distributed in space (Fig. 4). After normalizing for density (correcting for the proportion of time that animals spend in or out of the governmentally designated protected areas), ~70% of high errors occurred outside protected areas (PA) (Fig. 4). Using a binomial test, high errors were significantly ($P < 0.01$) more likely to occur outside PA boundaries for six elephants. One elephant demonstrated significantly more error within protected areas, while the remainder showed higher error outside the park, but not significantly (see Appendix: Fig. A7 for error maps of individual elephants). More strikingly, high errors clustered near the park boundaries, and especially in regions immediately neighboring villages. Most of the villages were never entered by the elephants (see "no-data" regions in black; Fig. 4), but the greatest clustering of inaccurate predictions was found to occur in the area overlapping with a particular village that was traversed by elephants moving in and out of the protected areas.

In addition to regions associated with human activity, low prediction accuracy coincided with areas of increased elevation and infrequent use. These results indicate that, in addition to avoiding areas with steep slopes (Wall et al. 2006), elephants exhibit qualitatively different movement behavior when ascending or descending and when traversing less familiar or avoided areas. It is likely that incorporating local elevation as a signal input would further improve prediction accuracy.

## DISCUSSION

### *Predicting elephant movement*

Although autocorrelation in movements was found to dominate the variability in hourly movements (Wittemyer et al. 2008), this study demonstrates that external stimuli exert greater influence over movement behaviors on larger timescales (weeks). The diurnal rhythms of elephants can be interpreted as somewhat constrained (due to movement and rest cycles), but the weekly excursion patterns resulting from varying environmental motivations are more complex. Such complexity limits the utility of CRW models to provide realistic predictions of animal movements. In answer to question 1, a filtering approach incorporating some information on landscape context or past behavior offers predictive power superior to that of a CRW model.

### *Elephant responses to the landscape*

Addressing question 2, our approach provided a powerful method to discern temporal and spatially

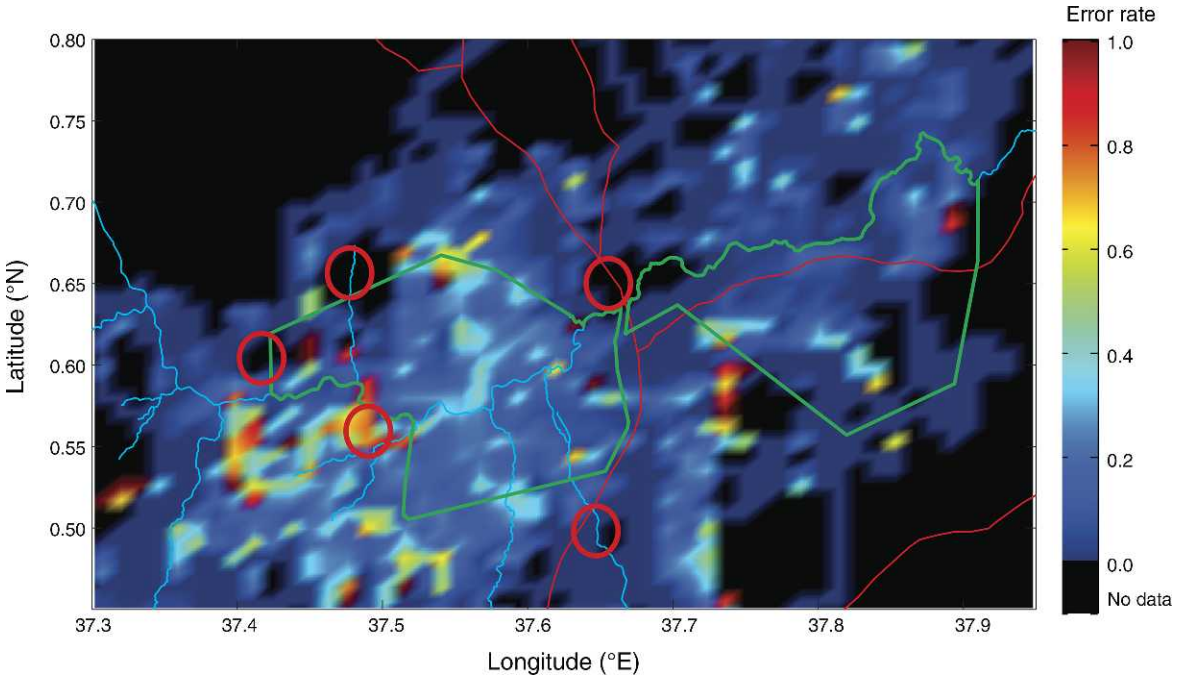


FIG. 4. A composite map of the relative error of filter predictions across the 13 elephants in the study ecosystem, providing insight to regions where unrecorded ecological features significantly impact elephant movements or nonlinear relationships between movements and signal inputs exist. The color key shows relative frequency of error (MSE $>$ 1.5). Interestingly, areas with high error (warmer colors) typically occur near the unfenced protected area boundaries (green-outlined polygons) and in proximity to human settlements (red open circles). Typically, elephants do not move directly through human settlement areas (black background denotes no location data), with one exception where error rates were high. Areas with high human activity were correlated with poor model predictions, suggesting that abnormal movements were associated with human encounters. Thin blue lines indicate the permanent rivers, and red lines indicate the roads.

specific relationships between movements and their ecological context. Importantly, our filtering approach is adept at assessing the predictive power of both static and dynamic features. Individual responses to landscape features were found to vary across space and time, as demonstrated by the relatively strong, but variable, predictive power of NDVI, the dynamic covariate signal input that has been shown to be a critical correlate of migratory behavior in other systems (Fryxell et al. 2005). Considering that areas with high NDVI are likely to have greater forage abundance or quality than areas with lower NDVI (Pettorelli et al. 2005), optimal elephant foraging strategies are hypothesized to result in chasing relatively high NDVI regions (Loarie et al. 2009). Therefore, it was surprising that individual strategies of movement in relation to NDVI varied dramatically across the 13 elephants studied (Appendix: Fig. A5) and movements were not significantly directed to areas with relatively higher NDVI. The utility of pursuing higher NDVI probably depends on dietary focus (Cerling et al. 2009, Wittemyer et al. 2009*a*) and vegetative structure (Young et al. 2009). Additionally, foraging strategies and spatial use are known to vary in relation to social factors (Wittemyer et al. 2007*a*, Wittemyer et al. 2008), making the creation of a general predictive framework complex.

Among static landscape features, distance to human features (protected area boundaries and roads) provided more information on movements than distance to permanent water. Human activities and roads are recognized to have dramatic effects on animal spatial behavior (Forman and Alexander 1998), with elephant-specific movement studies showing strong influences of roads (in central Africa; Blake et al. 2008) and protected area boundaries (Wittemyer et al. 2007*a*, 2008). The relatively weak predictive power of distance to water may relate more to the preprocessing of movements into 24-h summaries, subsuming the daily movements to and from water, as the distribution and movement of water-dependent elephants in the semiarid study system are strongly shaped by water (Wittemyer et al. 2007*a*).

### *Differentiated individual movement strategies*

The assessment of the uniformity of individual behavior is critical to a predictive framework. Although results from this study give insight to the relative importance of covariates for predicting elephant movement, information critical for in situ management, a general elephant movement predictive filter is unlikely to be effective. Specific to question 3, individual responses to the same features varied in time and space, rendering performance of a general filter weak, even when derived

from and applied to the same individual. Application of a filter derived from one elephant to another provided even less predictive utility. Elephants are complex animals (Moss 1988, Shoshani 1998, Wittemyer et al. 2005), which probably results in the observed differentiation in their responses to the same stimuli across time and space. Considering that the 13 tracked elephants in this study were part of larger groups, heterogeneity in behavioral influences from the myriad of group participants adds further complication to general predictions. Species with greater constraints on their movement strategies (e.g., navigation to a common target) or that are reliant on interspecific coordination (e.g., selfish herding) may be more amenable to general predictive monitoring using this framework (Codling et al. 2007).

*Insights from exploring properties of predictive error*

Despite the inability to derive a general filter for predicting elephant movement, mapping out error values provided insight to important aspects of the ecosystem not included in our model (e.g., topography) and helped to identify factors, including human habitation, that disrupt otherwise locally characterizable movement patterns. Although the largest errors appeared to be well-distributed in time, they were spatially clustered near, but outside, protected area boundaries in the open (unfenced) ecosystem. Previous work has demonstrated shifts to nocturnal access of permanent water outside protected areas in contrast to midday use, when elephants are within protected areas, presumably to avoid interference with humans and livestock (Wittemyer et al. 2007*a*). Here we found that movements of elephants in these human-dominated landscapes were much more difficult to predict, probably because movement behavior was reactive to the presence, movements, and threats of humans and livestock in such areas. This suggests that analysis of predictive model error is a potentially powerful tool for identifying areas in which a population faces threats (important for land use planning and reserve design) or for identifying factors that may be perturbing individuals.

*A model framework that advances movement ecology*

This study demonstrates that linear filtering offers a statistically robust framework for addressing the ecological questions posited in the *Introduction* that are critical to understanding the connections between environmental factors and movement behavior. The approach also provides a general framework for exploiting very large, multidimensional data sets in a computationally efficient manner to probe such interactions. Although state-space models, which explicitly infer relationships through a process model, have been lauded as the most promising approach for movement ecological research (Patterson et al. 2008, Schick et al. 2008), signal processing as applied here provides a correlative-based approach (bearing in mind that $\mathbf{d}[n]$ represents a movement state vector) that is able to reinforce and expand our understanding of movement properties and their relationship to landscape variables without any ab initio assumptions about the relevance or effects of those landscape variables (necessary in the state-space models described by Patterson et al. 2008). By their ability to distinguish dominant environmental covariates from peripheral ones, the signal-processing class of models can provide a rigorous approach to identifying factors that may then help to formulate more mechanistically detailed state-space models in the future.

## Acknowledgments

A. N. Boettiger and G. Wittemyer contributed equally to this work. This research was supported by NSF GRFP (A. N. Boettiger) and NIH grant GM083863-01 and USDI FWS Grant 98210-8-G745 to W. M. Getz. Fieldwork was hosted by the Save the Elephants Research Centre in Samburu, and movement data came from the Save the Elephants Tracking Animals for Conservation Program. We thank the Kenyan Office of the President, the Kenya Wildlife Service (KWS), and the Samburu and Buffalo Springs National Reserve's County Council, wardens, and rangers for their support of our work.

## Literature Cited

Barkham, J. P., and M. E. Rainy. 1976. Vegetation of Samburu-Isiolo Game Reserve. East African Wildlife Journal 14:297–329.

Bartumeus, F., J. Catalan, G. M. Viswanathan, E. P. Raposo, and M. G. E. da Luz. 2008. The influence of turning angles on the success of non-oriented animal searches. Journal of Theoretical Biology 252:43–55.

Berger, J. 2004. The last mile: How to sustain long-distance migration in mammals. Conservation Biology 18:320–331.

Bergman, C. M., J. A. Schaefer, and S. N. Luttich. 2000. Caribou movement as a correlated random walk. Oecologia 123:364–374.

Blake, S., S. L. Deem, S. Strindberg, F. Maisels, L. Momont, I.-B. Isia, I. Douglas-Hamilton, W. B. Karesh, and M. D. Kock. 2008. Roadless wilderness area determines forest elephant movements in the Congo Basin. PLoS ONE 3(10):e3546. [doi:10.1371/journal.pone.0003546]

Blanc, J. J., R. F. W. Barnes, C. G. Craig, H. T. Dublin, C. R. Thouless, I. Douglas-Hamilton, and J. A. Hart. 2007. African elephant status report, 2007: An update from the African elephant database. IUCN/SSC [International Union for the Conservation of Nature, Species Survival Commission] African Elephant Specialist Group, Gland, Switzerland.

Bowler, D. E., and T. G. Benton. 2005. Causes and consequences of animal dispersal strategies: relating individual behaviour to spatial dynamics. Biological Reviews 80:205–225.

Cerling, T. E., G. Wittemyer, J. R. Ehleringer, C. H. Remien, and I. Douglas-Hamilton. 2009. History of Animals using Isotope Records (HAIR): A 6-year dietary history of one family of African elephants. Proceedings of the National Academy of Sciences USA 106:8093–8100.

Codling, E. A., J. W. Pitchford, and S. D. Simpson. 2007. Group navigation and the "many-wrongs principle" in models of animal movement. Ecology 88:1864–1870.

Dalziel, B. D., J. M. Morales, and J. M. Fryxell. 2008. Fitting probability distributions to animal movement trajectories: Using artificial neural networks to link distance, resources, and memory. American Naturalist 172:248–258.

Douglas-Hamilton, I., T. Krink, and F. Vollrath. 2005. Movements and corridors of African elephants in relation to protected areas. Naturwissenschaften 92:158–163.

Edwards, A. M., R. A. Phillips, N. W. Watkins, M. P. Freeman, E. J. Murphy, V. Afanasyev, S. V. Buldyrev,

M. G. E. da Luz, E. P. Raposo, H. E. Stanley, and G. M. Viswanathan. 2007. Revisiting Levy flight search patterns of wandering albatrosses, bumblebees and deer. Nature 449:1044–1048.

Forman, R. T. T., and L. E. Alexander. 1998. Roads and their major ecological effects. Annual Review of Ecology and Systematics 29:207–231.

Fryxell, J. M., M. Hazell, L. Borger, B. D. Dalziel, D. T. Haydon, J. M. Morales, T. McIntosh, and R. C. Rosatte. 2008. Multiple movement modes by large herbivores at multiple spatiotemporal scales. Proceedings of the National Academy of Sciences USA 105:19114–19119.

Fryxell, J. M., J. F. Wilmshurst, A. R. E. Sinclair, D. T. Haydon, R. D. Holt, and P. A. Abrams. 2005. Landscape scale, heterogeneity, and the viability of Serengeti grazers. Ecology Letters 8:328–335.

Getz, W. M., and D. Saltz. 2008. A framework for generating and analyzing movement paths on ecological landscapes. Proceedings of the National Academy of Sciences USA 105:19066–19071.

Hayes, M. H. 1996. Statistical digital signal processing and modeling. Wiley, New York, New York, USA.

Hebblewhite, M., E. Merrill, and G. McDermid. 2008. A multi-scale test of the forage maturation hypothesis in a partially migratory ungulate population. Ecological Monographs 78:141–166.

Holdo, R. M., R. D. Holt, and J. M. Fryxell. 2009. Opposing rainfall and plant nutritional gradients best explain the wildebeest migration in the Serengeti. American Naturalist 173:431–445.

Johnson, A. R., J. A. Wiens, B. T. Milne, and T. O. Crist. 1992. Animal movements and population dynamics in heterogeneous landscapes. Landscape Ecology 7:63–75.

Kareiva, P. M., and N. Shigesada. 1983. Analyzing insect movement as a correlated random walk. Oecologia 56:234–238.

Lam, C. H., A. Nielsen, and J. R. Sibert. 2008. Improving light and temperature based geolocation by unscented Kalman filtering. Fisheries Research 91:15–25.

Lima, S. L., and P. A. Zollner. 1996. Towards a behavioral ecology of ecological landscapes. Trends in Ecology and Evolution 11:131–135.

Loarie, S. R., R. J. Van Aarde, and S. L. Pimm. 2009. Fences and artificial water affect African savannah elephant movement patterns. Biological Conservation 142:3086–3098.

Moss, C. J. 1988. Elephant memories: thirteen years in the life of an elephant family. William Morrow, New York, New York, USA.

Mueller, T., and W. F. Fagan. 2008. Search and navigation in dynamic environments—from individual behaviors to population distributions. Oikos 117:654–664.

Patterson, T. A., L. Thomas, C. Wilcox, O. Ovaskainen, and J. Matthiopoulos. 2008. State-space models of individual animal movement. Trends in Ecology and Evolution 23:87–94.

Pettorelli, N., J. O. Vik, A. Mysterud, J. M. Gaillard, C. J. Tucker, and N. C. Stenseth. 2005. Using the satellite-derived NDVI to assess ecological responses to environmental change. Trends in Ecology and Evolution 20:503–510.

Preisler, H. K., A. A. Ager, B. K. Johnson, and J. G. Kie. 2004. Modeling animal movements using stochastic differential equations. Environmetrics 15:643–657.

Royer, F., and M. Lutcavage. 2008. Filtering and interpreting location errors in satellite telemetry of marine animals. Journal of Experimental Marine Biology and Ecology 359:1–10.

Sanderson, E. W., M. Jaiteh, M. A. Levy, K. H. Redford, A. V. Wannebo, and G. Woolmer. 2002. The human footprint and the last of the wild. BioScience 52:891–904.

Schick, R. S., S. R. Loarie, F. Colchero, B. D. Best, A. Boustany, D. A. Conde, P. N. Halpin, L. N. Joppa, C. M. McClellan, and J. S. Clark. 2008. Understanding movement data and movement processes: current and emerging directions. Ecology Letters 11:1338–1350.

Shoshani, J. 1998. Understanding proboscidean evolution: a formidable task. Trends in Ecology and Evolution 13:480–487.

Sibert, J. R., M. K. Musyl, and R. W. Brill. 2003. Horizontal movements of bigeye tuna (*Thunnus obesus*) near Hawaii determined by Kalman filter analysis of archival tagging data. Fisheries Oceanography 12:141–151.

Simpson, S. J., G. A. Sword, P. D. Lorch, and I. D. Couzin. 2006. Cannibal crickets on a forced march for protein and salt. Proceedings of the National Academy of Sciences USA 103:4152–4156.

Turchin, P. 1991. Translating foraging movements in heterogeneous environments into the spatial distribution of foragers. Ecology 72:1253–1266.

Wall, J., I. Douglas-Hamilton, and F. Vollrath. 2006. Elephants avoid costly mountaineering. Current Biology 16:R527–R529.

Wittemyer, G., T. E. Cerling, and I. Douglas-Hamilton. 2009*a*. Establishing chronologies from isotopic profiles in serially collected animal tissues: An example using tail hairs from African elephants. Chemical Geology 267:3–11.

Wittemyer, G., I. Douglas-Hamilton, and W. M. Getz. 2005. The socioecology of elephants: analysis of the processes creating multitiered social structures. Animal Behaviour 69:1357–1371.

Wittemyer, G., W. M. Getz, F. Vollrath, and I. Douglas-Hamilton. 2007*a*. Social dominance, seasonal movements, and spatial segregation in African elephants: a contribution to conservation behavior. Behavioral Ecology and Sociobiology 61:1919–1931.

Wittemyer, G., J. B. A. Okello, H. B. Rasmussen, P. Arctander, S. Nyakaana, I. Douglas-Hamilton, and H. R. Siegismund. 2009*b*. Where sociality and relatedness diverge: the genetic basis for hierarchical social organization in African elephants. Proceedings of the Royal Society B 276:3513–3521.

Wittemyer, G., L. Polansky, I. Douglas-Hamilton, and W. M. Getz. 2008. Disentangling the effects of forage, social rank, and risk on movement autocorrelation of elephants using Fourier and wavelet analyses. Proceedings of the National Academy of Sciences USA 105:19108–19113.

Wittemyer, G., H. B. Rasmussen, and I. Douglas-Hamilton. 2007*b*. Breeding phenology in relation to NDVI variability in free-ranging African elephant. Ecography 30:42–50.

Young, K. D., S. M. Ferreira, and R. J. van Aarde. 2009. Elephant spatial use in wet and dry savannas of southern Africa. Journal of Zoology 278:189–205.

## APPENDIX

Computational implementation of data preprocessing, signal-processing framework, error calculation, and assessment of filter performance across individuals and models, and discussion of biological insights from evaluation of model structure (*Ecological Archives* E092-139-A1).

## SUPPLEMENT

MATLAB analysis code (*Ecological Archives* E092-139-S1).

*Ecological Archives* **E092-139-A1**

# Alistair N. Boettiger, George Wittemyer, Richard Starfield, Fritz Volrath, Iain Douglas-Hamilton, and Wayne M. Getz. 2011. Inferring ecological and behavioral drivers of African elephant movement using a linear filtering approach. *Ecology* 92:1648–1657.

Appendix A. Additional details on the computational implementation of data pre-processing, the signal processing framework, error calculation, and the assessment of filter performance; discussion of biological insights gained from evaluation of the model structure; figures depicting both methods and results as referenced in the main document; and two tables containing empirical results of filter performance across individuals and models.

## Computational implementation of data pre-processing and filtering

*Additional description of input data processing*

A simple lookup table provided the distances from rivers, roads and park boundaries at any point as a single scalar value. For prediction purposes we used only the elephant's absolute distance from any of these features. Elevation was used only to exclude regions effectively inaccessible to elephants, based on previous work demonstrating the study elephants avoid high angle slopes (Wall *et al.* 2006). Specifically, we modified our NDVI map to exclude data from all regions with greater than 20° slope, assuming the availability of resources and distance to other landscape features in these regions had no effect on elephant behavior.

Assuming elephant do not have ubiquitous knowledge of ecological conditions in their environs, we only included NDVI values within a 6 kilometer radius of an elephant's current position in our model. In order to remove data gaps (caused by missing data due to cloud cover or excluded in relation to slope) and limit processing requirements, these data were averaged in nine sub-sampled sectors defined as the area within a 1 km radius of the elephant's position (i.e. the local conditions) and 8 equal radial sectors out to the 6 km radius boundary (i.e. the conditions in possible movement directions; Fig. A2). Local vegetation scores compiled as the NDVI average values in the nine sectors were then included in the model as a nine dimensional vector.

*Signal processing framework extended*

In this section we explain in more detail the filtering prediction approach used. This is an application of a general technique for predicting the future behavior of an unknown stationary stochastic process from the statistical information in the signal. The basic theory for the discrete filter approach was laid down simultaneously by famous mathematicians Norbert Wiener and Andrey Kolmorgov in the 1940s. A more detailed introduction to Weiner filtering and its traditional applications can be found in most advanced texts on signal processing, Hayes 1996 provides an excellent treatment with the same notational conventions we employ. Let $d(t)$ be the real movement behavior. Let $s(t)$ be the signal input we can measure. Define the linear estimate of the values time $f$ in the future, of $d(t+f)$ as the estimate $d^*(t)$. We are looking for an optimal linear filter that will compute this value:

$$d^*(t) = L[d(t+f)|s(u), -\infty < u < t] \quad \text{(A.1)}$$

Here $L[\cdot]$ denotes the linear estimator. By convention, the estimated quantity (the stochastic variable *d*) is listed before the | symbol and the given quantities and constraints for the estimation (the stochastic variable *s* at all previous times) are listed after. If we insist that the filter is shift invariant, (depends only on the time of the observation s relative to the time at which we want to predict, rather than having explicit time dependence), the linear estimator can be written as a convolution:

$$d^*(t) = \int_0^\infty w(u)s(t-u)du \quad \text{(A.2)}$$

The task is to choose the function $w(t)$ such that the *expected* (squared) difference between the prediction we make about the future, $d^*(t)$, and the actual movement characteristics in the future $d(t+f)$, is minimized. We emphasize expected difference since both $d$ and $d^*$ are random variables.

Let $e(t)= d^*(t)– d(t+f)$ be our error at time $t$. We want to minimize the mean squared error, $\mathrm{E}[e(t)^2]$ (where $\mathrm{E}[x] = \int_0^\infty xp(x)dx$), the expectation value of the random variable $x$ defined by the probability density function $p(x)$). This is achieved when the error, $e(t)$ is orthogonal to the observations $s(t)$. A $w(t)$ for which the error is still correlated with the input signals suggests that some of that error signal actually contains information we could be using in our prediction. The function $w(t)$ which satisfies this orthogonality criteria is called a Weiner filter. Mathematically we can write the orthogonality condition as,

$$\mathrm{E}[e(t)s(t)] = 0 \quad \text{(A.3)}$$

substituting in for $e(t)$

$$\mathrm{E}\big[\big(d^*(t) - d(t+f)\big)s(t)\big] = 0 \quad \text{(A.4)}$$

and substituting Eq. A.2 into this

$$\mathrm{E}\big[\int_0^\infty w(u)s(t-u)du - d(t+f)s(t)\big] = 0 \quad \text{(A.5)}$$

The expectation operator is linear and we can distribute it over the arguments and change the order with the integration, resulting in

$$\int_0^\infty w(u)\mathrm{E}[s(t-u)s(t)]du - \mathrm{E}[d(t+f)s(t)] = 0 \quad \text{(A.6)}$$

$\mathrm{E}[s(t-u)s(t)]$ is just the auto correlation in $s$, $r_s(t-u)$, and $\mathrm{E}[d(t+f)s(t)]$ is the cross correlation $r_{ds}(t+f)$. So we can rewrite Eq. A.6 as:

$$\int_0^\infty w(u)r_s(t-u)du = r_{ds}(t+f) \quad \text{(A.7)}$$

Equations of this form are called Weiner-Hopf equations. $r_{ds}$ and $r_s$ can be computed from the statistics of the measurements $s$, and the movements, $d$, and therefore Eq. A.7 can be solved for the optimal $w$. The solution approach for this continuous time predictive Weiner filter can be found in many standard texts on statistical signal processing, (eg. Hayes 1996).

Since we have real data sampled at discrete intervals the convolutions can be written as sums. If we restrict the filter to only using signals from time $t-p$ until now, (i.e. $p$ samples ago rather than from – infinity ago), these become finite sums and can be written as matrix products.

$$d[n] = \sum_{k=0}^{p-1} w[k]s[n-k] \tag{A.8}$$

Solving the discrete Wiener-Hopf equations (A.8) for w defines the optimal linear filter we are seeking. There are several ways this can be done, for computational efficiency we rephrase Eq. A.8 as a matrix equation which can then be solved by matrix inversion.

The derivation also readily generalizes to multidimensional signal inputs, $\boldsymbol{s}[n]$ and multidimensional data $\boldsymbol{d}[n]$, where the components of $\boldsymbol{d}[n]$ (e.g. x-centroid of movement, angle of movement) are indexed by $j$ and the components of the signal (e.g. vegetation, distance from water, previous movement) are indexed by $i$.

$$d_j[n] = \sum_{i=1}^{N} \sum_{k}^{p-1} W_{i,j}[k]s_i[n-k] \tag{A.9}$$

To solve the discrete, multidimensional Weiner-Hopf equations in (A.9), we rewrite this equation in matrix form. Eq. A.9 is the same as Eq. 1 in the main text. Choosing $p$=5, for reasons elaborated below, and $N$=17 (using all available signals) gave the best results.

Let $\mathbf{W}^*$ be *a* $pN$ x 4 with 4 columns for each of the 4 movement characteristics $j$, defined as:

$$\mathbf{W}_j^* = \left[\left[W_{1j}[k] \ldots W_{Nj}[k]\right] \ldots \left[W_{1j}[k-p] \mathrm{K} W_{Nj}[k-p]\right]\right]^T \tag{A.10}$$

for columns $j$=1:4. Note the time dependence of $\mathbf{W}[n]$ has been re-arranged into the explicit elements of the larger matrix $\mathbf{W}^*$, whose components are not time dependent variables. Let $\mathbf{R}_s$ be a $pN$ x $pN$ matrix, which is an $N$ x $N$ array of $p$ x $p$ sub matrices for the autocorrelations and cross correlations of the signals evaluated for separations of up to $p$. Finally, let $\mathbf{R}_{ds}$ be a $pN$ x 4 matrix where the columns again correspond to each of the movement characteristics, $j$, as for $\mathbf{W}^*$, and each $p$ entries correspond to the discretely sampled cross correlation of characteristic $j$ with input signal $i$=*1:N*. Each of the $j$ columns is therefore:

$$[\mathbf{R}_{ds}]_j = \left[\left[r_{d_j s_1}[k] \ldots r_{d_j s_N}[k]\right] \ldots \left[r_{d_j s_1}[k-p] \mathrm{K} r_{d_j s_N}[k-p]\right]\right]^T \tag{A.91}$$

for columns $j$=1:4. Then the multidimensional sum in equation (A.9) can be readily written as the matrix product, $\mathbf{R}_s\mathbf{W}^* = \mathbf{R}_{ds}$, from which $\mathbf{W}^*$ is readily solved by inverting $\mathbf{R}_s$ and multiplying through by that result:

$$\mathbf{W}^* = \mathbf{R}_s^{-1}\mathbf{R}_{ds} \tag{A.102}$$

From which the coefficients of $\mathbf{W}[k]$ can be read out following Eq. A.10.

*Error calculation details extended*

Filter performance was assessed through the calculation of the mean squared error (MSE) of the position of predicted movements relative to actual movements. Because signal power varied over time, MSE was normalized by the root power of the signal (i.e. standard deviation). As a result

of these normalization processes, MSE units are not directly translatable to a straight metric of spatial accuracy (i.e. the difference in meters of predicted from actual movements). Therefore, comparisons represent relative differences in performance. In order to provide a conceptual understanding of filter performance, simplified representation of predictive movement error is presented in the form of the actual spatial error (km) of the CoM. In order to do this, CoM error is calculated independently from the other movement parameters and presented alongside the normalized error for the overall filter in Table 1. Comparison of representative predictions and actual movements that correspond to the median MSE are shown in Fig. 1.

*Additional information regarding assessment of filter performance*

Comparison within and across elephants was restricted in relation to absolute time, season, and/or location. Restrictions in relation to time were straightforward. Restrictions in relation to season or NDVI were conducted simply by requiring the NDVI value for the starting point of the elephant whose movement we aimed to predict with a different filter was within 20% of the relative range of the NDVI value for the starting point of the dataset from which the filter was constructed (e.g. if the NDVI data is normalized from 0 to 1, the difference in the NDVI values could be no more than 0.2). For the location-based restriction, the distance between the two starting data points had to be within 20% of the total latitude and longitudinal range visited by any of the 13 elephants in our data set. Differences in data sets across the elephants limited the application of filters across elephants at the same time, with samples sizes of a 'same time different elephant' analysis varying widely across pairs with multiple pairs lacking any comparison. Therefore, results of such an analysis were not presented. In addition, certain similarity constraints between the datasets for a given pair of elephants had little or no overlap. If the amount of overlapping data was less than 25% of the median number of overlapping data sets for that set of criteria, the results were excluded as not statistically robust.

To test for possible relationships between local landscape features and locations where filter predictions are generally poor, we divided the study region into 100 x 100 meter grid sections. Within each section, we computed the number times an elephant was present and a motion prediction was made, and the number of times the prediction had significant error. The number of errors was normalized by the number of total predictions made in each section, and recorded as the error density. Results were plotted in a linear colormap where red indicates the highest error rate observed, blue the lowest, and black indicates no data. The choice of the cutoff for ‘significant error’ was defined as MSE of 1.5, a level which exceeds the performance of a random walk but nonetheless shows considerable deviation from the average prediction using all environmental inputs. Different error cutoffs affected the data density and statistical confidences in the resulting error map, rather than the spatial pattern of errors (see Fig. A8 for error map with error as greater than MSE 2.7).

**Insights from Model Structure**

Our use of the Wiener filter illustrates how scales of analysis can be bridged (a focus of some research, e.g. Fryxell et al. 2008) by taking data that has already been analyzed in the context of diurnal autocorrelation patterns recognized to dominate variance in hourly movements (Wittemyer et al 2007) and compressing it into a daily representation. This was accomplished not

simply as a single average location, but through the device of a bounding ellipse characterized by four parameters. As such, the computational burden of using the raw data itself was reduced, but information about the directionality and dispersion of the daily movement was retained. Similarly, our reduction of NDVI information using an inter-spoke and wheel approach also reduced the computational burden of our approach. These preprocessing steps thereby allowed us to focus on larger scale movement properties and provided comprehensive assessment of the performance of our models in several different contexts (e.g. across time and space, and among individuals).

The temporal efficiency of filter fitting and prediction was compared across input and predictive data scales of four orders of magnitude (from 10s tens to 10000s of hours; Fig. A3). Optimal performance occurred at around 6 weeks (500 hours for preprocessing and 500 hours for prediction). Filter fits at shorter time intervals did not perform well, while non-stationarity in longer-term datasets degraded longer period performance. Short-term shifts in foraging/land-use strategies potentially drive inaccurate estimates of correlation functions at this temporal resolution, as occurred when an elephant went in and out of the protected areas (Fig. 4). Similarly, non-stationary movement behavior at longer time scales (2+ months) reduced predictability, probably in relation to ecological changes in the biannual rainy season system (dry to wet transitions are graded over 3 month periods) and resulting range shifts (Wittemyer 2008). As such, this approach provided reasonably good insights regarding the correlates of movement at monthly time scales, but the implementation of this method to predict and understand covariates driving movement across seasonal or annual transitions appears limited.

## Appendix Literature Cited:


Hayes, M. H. 1996. *Statistical digital signal processing and modeling*. Wiley, New York.

Fryxell, J. M., M. Hazell, L. Borger, B. D. Dalziel, D. T. Haydon, J. M. Morales, T. McIntosh, and R. C. Rosatte. 2008. Multiple movement modes by large herbivores at multiple spatiotemporal scales. Proceedings of the National Academy of Sciences of the United States of America **105**:19114-19119.

Stoffer, D.S. and Shumway, R. H. *Time Series Analysis and Its Applications*. Springer, 2000.

Wall, J., Douglas-Hamilton, I., and Vollrath, F. Elephants avoid costly mountaineering. Current Biology, 16:R527–R529, 2006.

Wittemyer, G., W. M. Getz, F. Vollrath, and I. Douglas-Hamilton. 2007. Social dominance, seasonal movements, and spatial segregation in African elephants: a contribution to conservation behavior. Behavioral Ecology and Sociobiology **61**:1919-1931.

Wittemyer, G., L. Polansky, I. Douglas-Hamilton, and W. M. Getz. 2008. Disentangling the

effects of forage, social rank, and risk on movement autocorrelation of elephants using Fourier and wavelet analyses. Proceedings of the National Academy of Sciences of the United States of America **105**:19108-19113.

**Fig. A1**

G.P.S. data were preprocessed to reduce the dimensionality of the movement input data in the Weiner filter model. All G.P.S. points recorded during each 24 hour period were simplified into a four parameter characterization of the daily movement consisting of the x and y coordinates of the center of mass, and the length and angle of the long axis of the minimum ellipse capturing all data in the 24 hour periods.

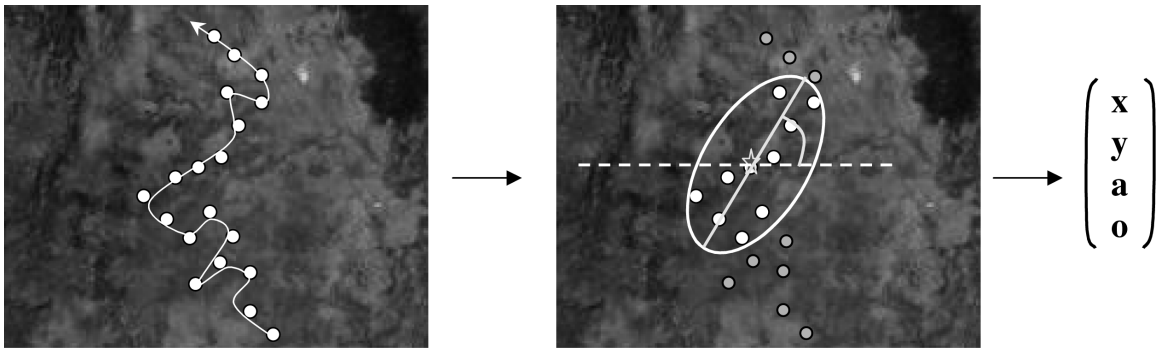


**Fig. A2**.

**A** Normalized Differential Vegetation Data (NDVI) were preprocessed to reduce the dimensionality of the vegetation dynamic input data in the Weiner filter model. **B** For each 24 hour moving window, NDVI within a 6 km radius of the center of mass was characterized as a nine parameter vector, ***g***. **C** Each component of ***g*** represents the average value within a 1 km radius centroid and 8 equal sized sectors radiating from the centroid to the bounding circle perimeter.

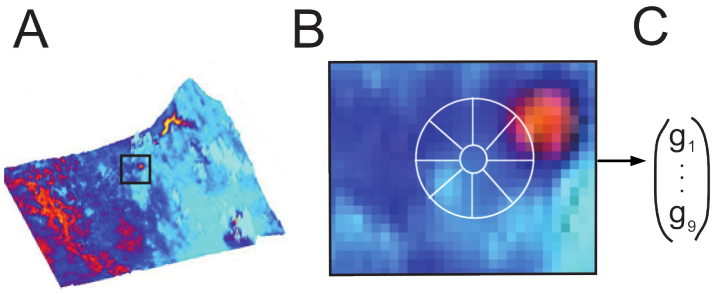

**Fig. A3**

Filter performance varied in relation to the amount of data input in the model. Optimal performance for the filter containing all signal inputs occurred using 1000 hours of data. The optimal amount of data varied slightly across specific input signals.

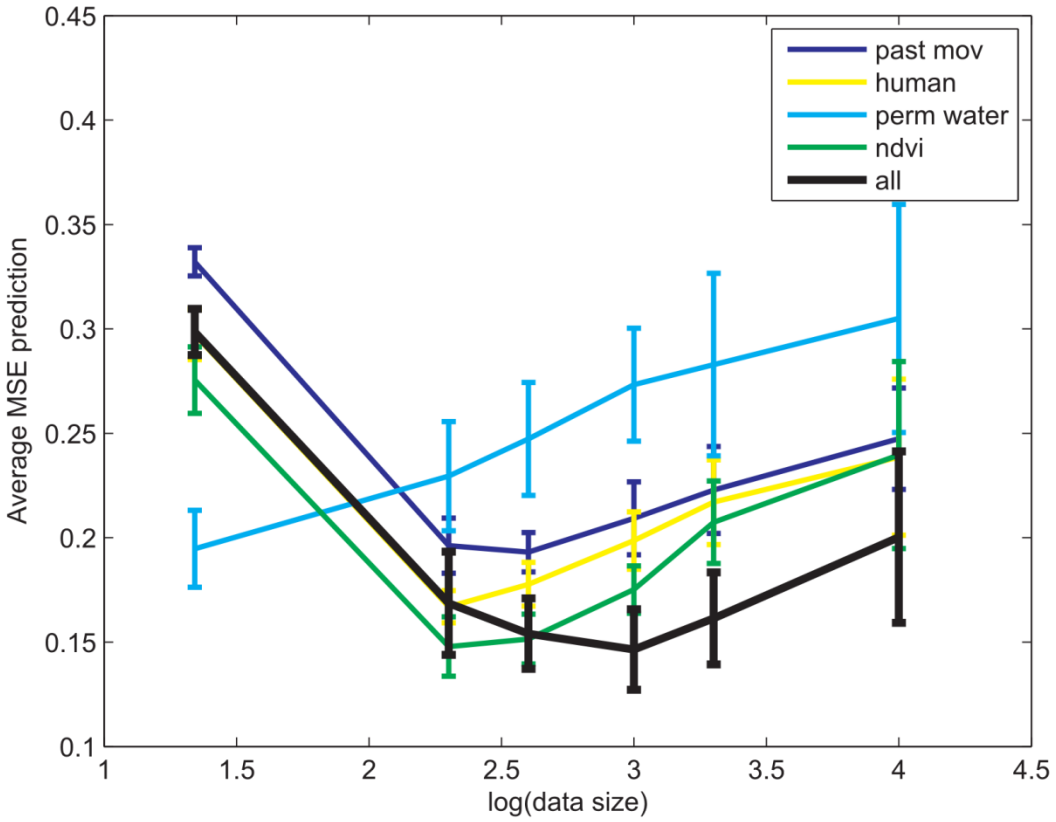

**Fig. A4**

Relative contributions, $r_i$, of past movement history, NDVI, and static features to model predictions for Anastasia. Computed as

$$r_i = \frac{MSE_i^{-1}}{\sum_i MSE_i^{-1}}$$

Note on a short time scale movement predictions are frequently dominated by one or two signals, and the others hold little predictive information. A similar degree of variation in predictive values is seen in the data for the other elephants.

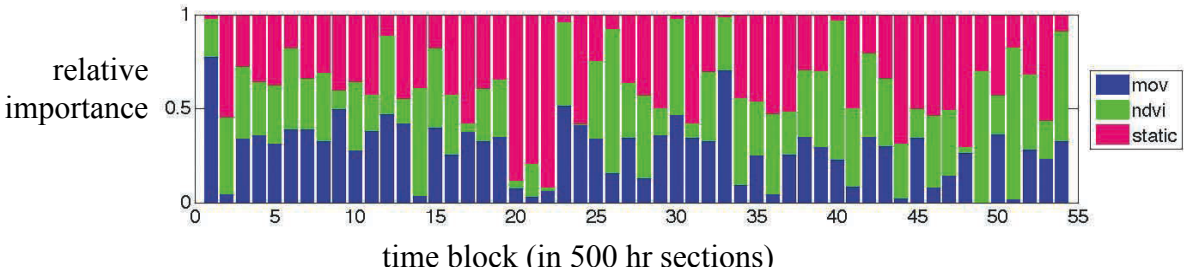

**Fig. A5**

The influence of dynamic vegetation productivity (as recorded by remotely sensed NDVI) was a key signal input in the Wiener filter. A histogram for each of the 13 elephants and all in combination (last panel) shows the relative frequency elephant movements remained in the same sector (left column) or moved to areas with differing relative NDVI values (second column to left is the sector with the highest NDVI progressing to the sector with the lowest NDVI to the right). The 8 sectors and NDVI ranking scheme are indicated in the inset, bottom right. The relationship between elephant movements and NDVI was dynamic, and showed marked differences across individuals. Some individuals demonstrated directed movements to higher NDVI while others show no in relation to NDVI.

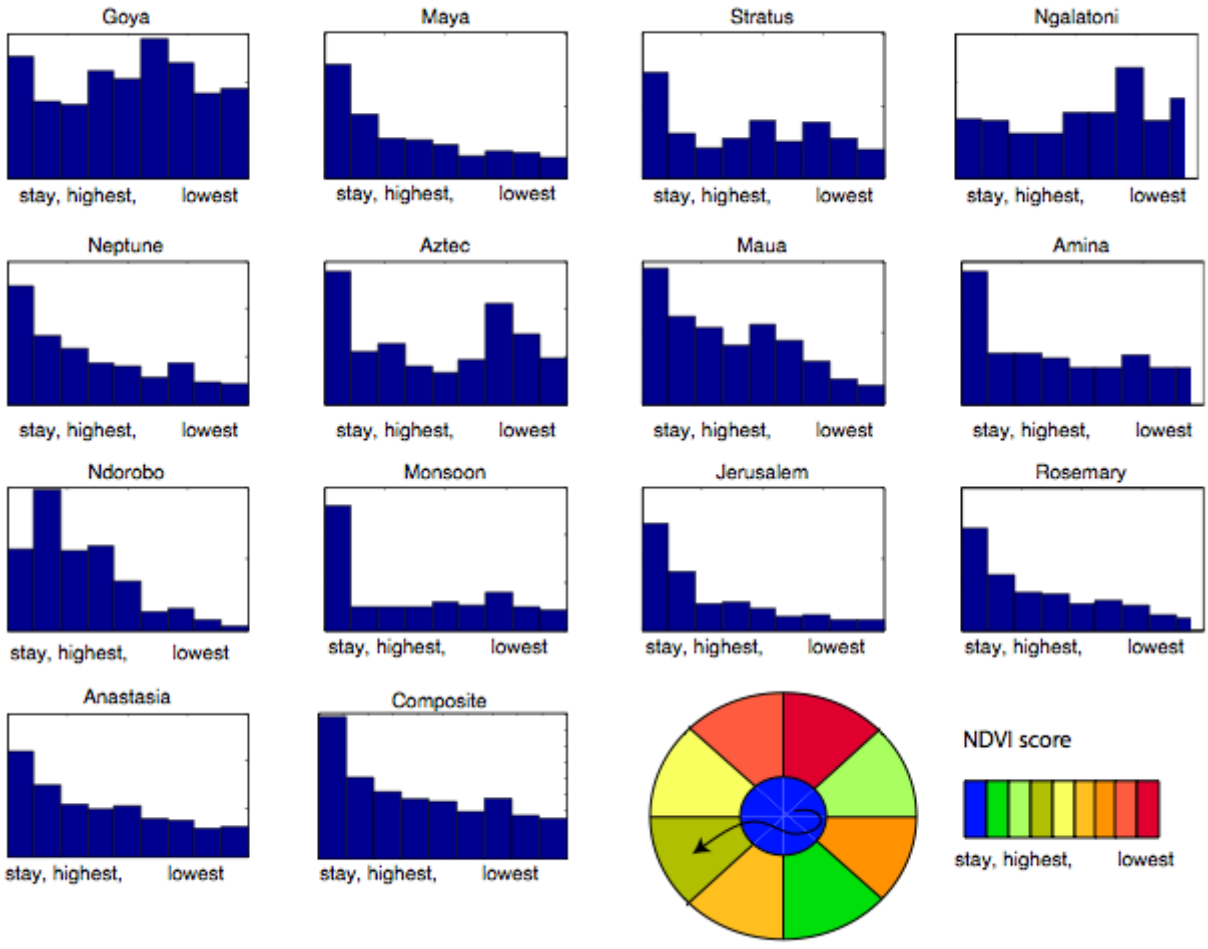

**Fig. A6**

Predictive performance of filters applied randomly or with time, season, and spatial constraints rather than applied to consecutive 500 hour period. Filter performance was greater when applied to the elephant from which it originated, with performance decreasing by ~30% when applied to a different elephant. Constraining the filter such that it was applied to data collected within 3 months (Time < 3), at relatively similar locations (Nearby: within 0.2 of normalized distance values) and under similar seasonal conditions (Season: < 0.2 on normalized NDVI scale) increased performance.

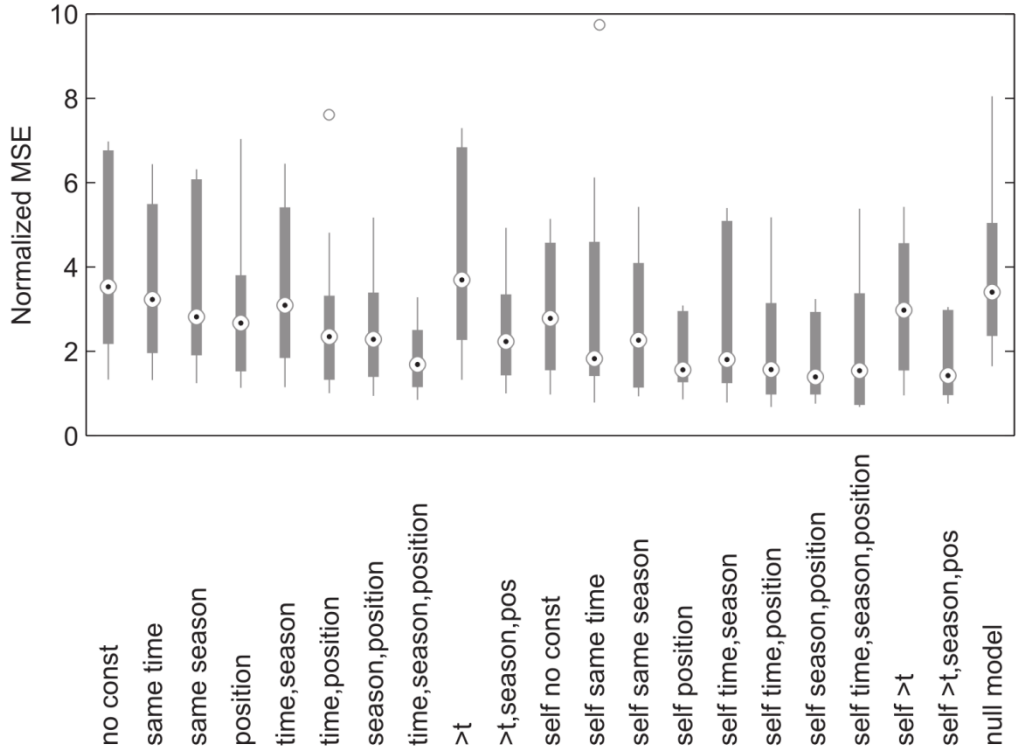

**Fig. A7**

Spatial error map with cut off equal to MSE of 2.7, a threshold value approaching the average performance of the null model. Results are qualitatively similar to those shown in the main body indicating the location and density of error was not a function of the threshold chosen in this analysis.

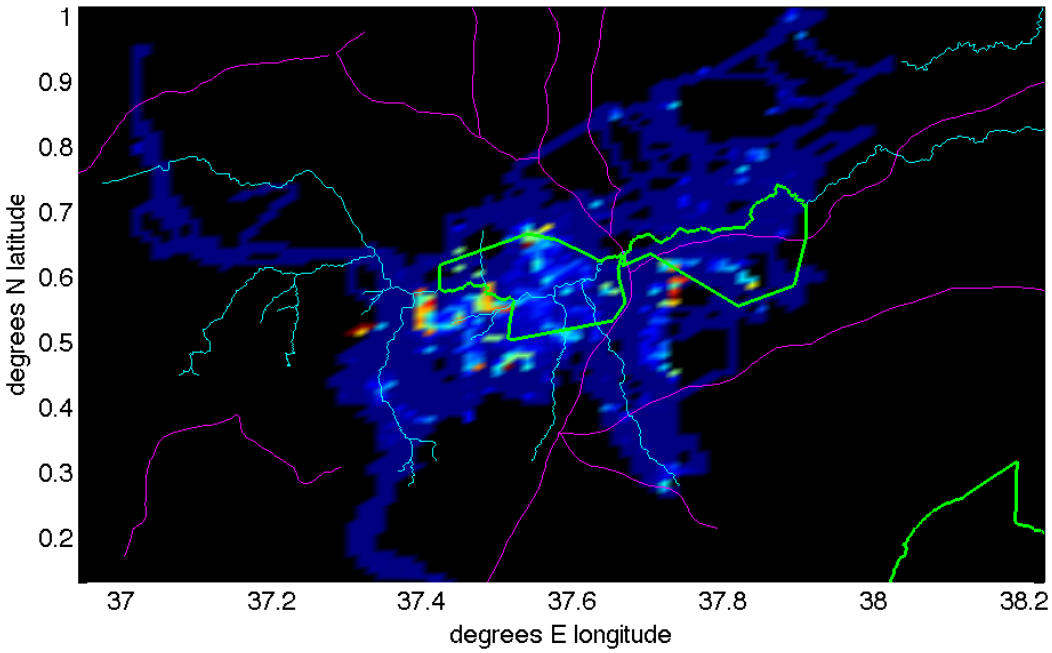

**Fig. A8**

Spatial error map of each individual elephant for which the combination is presented in Fig. 4. Different individuals demonstrates stark differences in ranging patterns and, in relation, the location of predictive error. Individuals which were found almost exclusively within protected areas typically demonstrate the greatest error within the PA boundaries (e.g. Aztec and Maua), though Goya shows the opposite relationship. Most other individuals demonstrate higher error outside PA boundaries, the specific location of which appeared to relate to the overlap between human activity and their home range.

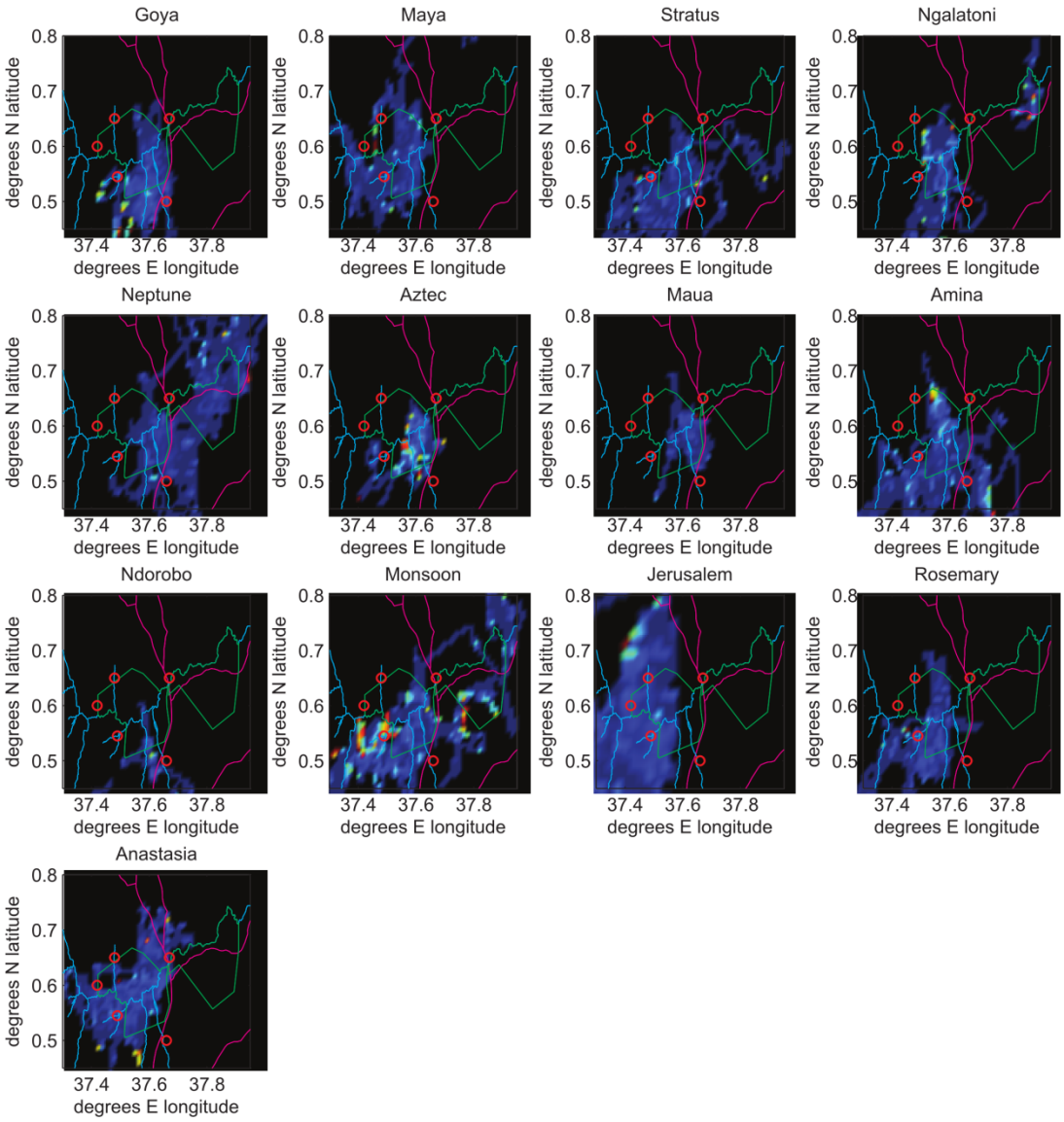

**Table A1**

The (normalized mean square error (MSE) of movement predictions across the 13 elephants were qualitatively similar. While elephants were tracked for different durations, tracking data covered different years and season, and movements were focused on different areas in the ecosystem, the best movement prediction (lowest MSE) was derived from the combination of all inputs regardless of elephant. Predictions using any signal input or combination of signal inputs exceeded those from the null model by an order of magnitude.

| | All | Movement | COM | NDVI | Static | Human | Water |
|---|---|---|---|---|---|---|---|
| **Goya** | 0.132 | 0.209 | 0.674 | 0.194 | 0.227 | 0.240 | 0.297 |
| **Maya** | 0.119 | 0.221 | 0.409 | 0.209 | 0.195 | 0.243 | 0.384 |
| **Stratus** | 0.116 | 0.242 | 0.367 | 0.253 | 0.493 | 0.377 | 0.427 |
| **Ngalatoni** | 0.133 | 0.238 | 0.388 | 0.348 | 0.277 | 0.298 | 0.615 |
| **Neptune** | 0.132 | 0.252 | 0.522 | 0.267 | 0.231 | 0.261 | 0.789 |
| **Aztec** | 0.119 | 0.240 | 0.721 | 0.254 | 0.518 | 0.326 | 0.333 |
| **Maua** | 0.131 | 0.245 | 0.389 | 0.192 | 0.210 | 0.219 | 0.806 |
| **Amina** | 0.123 | 0.298 | 0.523 | 0.237 | 0.269 | 0.341 | 0.601 |
| **Ndorobo** | 0.122 | 0.209 | 0.365 | 0.172 | 0.236 | 0.774 | 0.375 |
| **Monsoon** | 0.133 | 0.242 | 0.349 | 0.264 | 0.194 | 0.270 | 0.462 |
| **Jerusalem** | 0.119 | 0.206 | 0.495 | 0.191 | 0.210 | 0.206 | 0.290 |
| **Rosemary** | 0.115 | 0.210 | 0.339 | 0.195 | 0.256 | 0.285 | 0.400 |
| **Anastasia** | 0.130 | 0.304 | 0.643 | 0.285 | 0.234 | 0.222 | 0.378 |

**Table A2**

Numerical values corresponding to Fig. A6, showing the predictive performance of filters applied randomly or with time, season, and spatial constraints rather than applied to consecutive 500 hour period. Here 'self' indicates that only filters made with data from elephant E are were used in predicting motion of elephant E.

| Constraints | Self<br>Median (IQR) | Across Elephant<br>Median (IQR) |
|---|---|---|
| No restrictions | 2.78 (1.52, 5.14) | 3.53 (2.15, 6.69) |
| Time>3 | 2.98 (1.51, 5.42) | 3.69 (2.19, 6.69) |
| Time<3 | 1.82 (1.41, 6.12) | 3.22 (1.50, 5.18) |
| Season | 2.26 (1.03, 5.42) | 2.81 (1.86, 6.00) |
| Nearby (<20%) | 1.56 (1.03, 2.99) | 2.67 (1.42, 3.50) |
| Season, Position | 1.39 (0.92, 2.02) | 2.28 (1.32, 3.18) |
| Time>3, Season, Position | 1.42 (0.92, 3.04) | 2.23 (1.33, 3.01) |
| Time<3, Season | 1.80 (1.03, 5.39) | 3.09 (1.43, 5.07) |
| Time<3, Position | 1.57 (0.80, 3.42) | 2.35 (1.27, 3.26) |
| Time<3, Season, Position | 1.54 (0.71, 3.88) | 1.69 (1.08, 2.42) |
| Null Model | 3.51 (2.98,5.71 ) | |

# Ecological Archives

## *Appendix B*

# Inferring ecological and behavioral drivers of African elephant movement using a linear filtering approach

Alistair Boettiger, George Wittemyer, Richard Starfield, Iain Douglas-Hamilton, Fritz Volrath, Wayne M. Getz

The Appendix contains the Matlab code for implementing the primary signal processing analysis using a Weiner filter. Additional code for the analyses implemented in the manuscript is available upon requests from the authors:
:

```
    %=================================================================%
    %                          Wiener Filter                          %
    %=================================================================%
 % Functionally Complete                          Last Modified: 08/21/09
 %
 % Wiener_filter_compsig.m
 %
 % loads data of normalized movement stats and normalized NDVI, chopped
 % into continuous time sections of a no more than the chosen segment
 % length (eg 1000 hours).  The first half of the data is used for choosing
 % the filter coefficients and the second half is used for evaluating
 % performance.
 %
 % E3i8  E10ss12
 %

  clear all;


names = {'Goya','Maya','Stratus','Ngalatoni','Neptune','Aztec','Maua',...
 'Amina','Ndorobo','Monsoon','Jerusalem','Rosemary','Anastesia'};

    K=13; % number of pachyderms
    M=5; % number of taps to use in Wiener filter
    Q=4; % number of output dimensions to predict
    relw = zeros(9,K); % average relative weights.  in classes x elephants

    ErrT = zeros(K,8);
    ErrM = zeros(K,8);
    ErrT2 = zeros(K,8);
    ErrM2 = zeros(K,8);
    ErrT3 = zeros(K,8);
    ErrM3 = zeros(K,8);
    Err_data = cell(8);
```

```
 for E= 1:K % 1:K
   load(['E_all3_', num2str(E), '_wiener']);
    S=length(sys_dat);    [Nt P] = size(sys_dat{1});
    ws = zeros(S,P); val = zeros(1,S);

 Err = zeros(S,8);
Err2 = zeros(S,8);
Err3 = zeros(S,8);


 % mse = NaN*ones(S,Q); % reinitialize data array
 for ss= 1:S % loop over sectors
     % ~~~~~~~~Filter using random input signals~~~~~~~~~~~~~~~~~~~~~%
     % Seperate input and output
        [Nt P] = size(sys_dat{ss});
        N = 2*floor(floor(Nt/2)/2); %split data set in half. N must be even
        X = rand(N,9);
        Y = sys_dat{ss}(end-N+1:end,1:Q);
% Initialize some Wiener Filter Parameters
[N,P]=size(X); [No,Q]=size(Y); W=zeros(M*P,Q); y_rand = zeros(No,Q);
% =============Start computing autocorrelation matrices================ %
    RX = xcorr(X,N/2,'unbiased'); R_X = {}; % compute correlation functions
    for i=1:P^2 % stack correlation functions into block Toeplitz corr.
matrices
         j= 1+floor((i-.2)/P);
         k =1+ mod(i-1,P) ;
        R_X{j,k} = toeplitz(RX(N/2+1:N/2+M,i));
    end
    R_X = cell2mat(R_X); % convert into big matrix.
          % figure(7); imagesc(R_X); colorbar;
    for q=1:Q % loop over output dimensions
        R_iy = zeros(P,M);
        for i=1:P % loop over input dimensions
            [c_iy, lags] = xcorr(X(1:No,i),Y(:,q),No/2,'unbiased') ;
            R_iy(i,:) = flipud(c_iy(No/2+2:No/2+M+1));
        end
            r_iy = reshape(R_iy',P*M,1)'; % cross correlation fxn
            W(:,q) =  (r_iy/R_X)';  % compute Weiner Filter Coefficients
        for i=1:P % loop over input dimensions
            y_t = conv(X(1:No,i),W(1+(i-1)*M:i*M,q));
            y_rand(:,q) = y_rand(:,q) + y_t(M:end); % actual prediction
        end
   end    % end loop over q
% ====================================================================== %
%~~~~~~~~~~~~~~~~~~~~~~~~~~~~~~~~~~~~~~~~~~~~~~~~~~~~~~~~~~~~~~~~~~~~~~~~%


% ~~~~~~~~Filter using just MOVEMENT input signals~~~~~~~~~~~~~~~~~~~~~%
     % Seperate input and output
        [Nt P] = size(sys_dat{ss});
        N = 2*floor(floor(Nt/2)/2); %split data set in half. N must be even
        X = sys_dat{ss}(1:N,1:4);
        Y = sys_dat{ss}(end-N+1:end,1:Q);
% Initialize some Wiener Filter Parameters
[N,P]=size(X); [No,Q]=size(Y); W=zeros(M*P,Q); y_mov = zeros(No,Q);
```

```
% =============Start computing autocorrelation matrices================ %
    RX = xcorr(X,N/2,'unbiased'); R_X = {}; % compute correlation functions
    for i=1:P^2 % stack correlation functions into block Toeplitz corr.
matrices
          j= 1+floor((i-.2)/P);
          k =1+ mod(i-1,P) ;
         R_X{j,k} = toeplitz(RX(N/2+1:N/2+M,i));
    end
    R_X = cell2mat(R_X); % convert into big matrix.
          % figure(7); imagesc(R_X); colorbar;
    for q=1:Q % loop over output dimensions
        R_iy = zeros(P,M);
        for i=1:P % loop over input dimensions
            [c_iy, lags] = xcorr(X(1:No,i),Y(:,q),No/2,'unbiased') ;
            R_iy(i,:) = flipud(c_iy(No/2+2:No/2+M+1));
        end
            r_iy = reshape(R_iy',P*M,1)'; % cross correlation fxn
            W(:,q) =  (r_iy/R_X)';  % compute Weiner Filter Coefficients
        for i=1:P % loop over input dimensions
            y_t = conv(X(1:No,i),W(1+(i-1)*M:i*M,q));
            y_mov(:,q) = y_mov(:,q) + y_t(M:end); % actual prediction
        end
   end    % end loop over q
% ========================================================================== %
%~~~~~~~~~~~~~~~~~~~~~~~~~~~~~~~~~~~~~~~~~~~~~~~~~~~~~~~~~~~~~~~~~~~~~~~~~~~~%

% ~~~~~~~~Filter using just COM input signals~~~~~~~~~~~~~~~~~~~~~%
     % Seperate input and output
        [Nt P] = size(sys_dat{ss});
        N = 2*floor(floor(Nt/2)/2); %split data set in half. N must be even
        X = sys_dat{ss}(1:N,1:2);
        Y = sys_dat{ss}(end-N+1:end,1:Q);
% Initialize some Wiener Filter Parameters
[N,P]=size(X); [No,Q]=size(Y); W=zeros(M*P,Q); y_com = zeros(No,Q);
% =============Start computing autocorrelation matrices================ %
    RX = xcorr(X,N/2,'unbiased'); R_X = {}; % compute correlation functions
    for i=1:P^2 % stack correlation functions into block Toeplitz corr.
matrices
          j= 1+floor((i-.2)/P);
          k =1+ mod(i-1,P) ;
         R_X{j,k} = toeplitz(RX(N/2+1:N/2+M,i));
    end
    R_X = cell2mat(R_X); % convert into big matrix.
          % figure(7); imagesc(R_X); colorbar;
    for q=1:Q % loop over output dimensions
        R_iy = zeros(P,M);
        for i=1:P % loop over input dimensions
            [c_iy, lags] = xcorr(X(1:No,i),Y(:,q),No/2,'unbiased') ;
            R_iy(i,:) = flipud(c_iy(No/2+2:No/2+M+1));
        end
            r_iy = reshape(R_iy',P*M,1)'; % cross correlation fxn
            W(:,q) =  (r_iy/R_X)';  % compute Weiner Filter Coefficients
        for i=1:P % loop over input dimensions
            y_t = conv(X(1:No,i),W(1+(i-1)*M:i*M,q));
            y_com(:,q) = y_com(:,q) + y_t(M:end); % actual prediction
        end
   end    % end loop over q
```

```
% ========================================================================= %
%~~~~~~~~~~~~~~~~~~~~~~~~~~~~~~~~~~~~~~~~~~~~~~~~~~~~~~~~~~~~~~~~~~~~~~~~~~%




% ~~~~~~~~Filter using just NDVI input signals~~~~~~~~~~~~~~~~~~~~~%
     % Seperate input and output
        [Nt P] = size(sys_dat{ss});
        N = 2*floor(floor(Nt/2)/2); %split data set in half. N must be even
        X = sys_dat{ss}(1:N,9:end-1);% NDVI inputs
        Y = sys_dat{ss}(end-N+1:end,1:Q);
% Initialize some Wiener Filter Parameters
[N,P]=size(X); [No,Q]=size(Y); W=zeros(M*P,Q); y_ndvi = zeros(No,Q);
% =============Start computing autocorrelation matrices================ %
    RX = xcorr(X,N/2,'unbiased'); R_X = {}; % compute correlation functions
    for i=1:P^2 % stack correlation functions into block Toeplitz corr.
matrices
          j= 1+floor((i-.2)/P);
          k =1+ mod(i-1,P) ;
         R_X{j,k} = toeplitz(RX(N/2+1:N/2+M,i));
    end
    R_X = cell2mat(R_X); % convert into big matrix.
          % figure(7); imagesc(R_X); colorbar;
    for q=1:Q % loop over output dimensions
        R_iy = zeros(P,M);
        for i=1:P % loop over input dimensions
            [c_iy, lags] = xcorr(X(1:No,i),Y(:,q),No/2,'unbiased') ;
            R_iy(i,:) = flipud(c_iy(No/2+2:No/2+M+1));
        end
            r_iy = reshape(R_iy',P*M,1)'; % cross correlation fxn
            W(:,q) =  (r_iy/R_X)';  % compute Weiner Filter Coefficients
        for i=1:P % loop over input dimensions
            y_t = conv(X(1:No,i),W(1+(i-1)*M:i*M,q));
            y_ndvi(:,q) = y_ndvi(:,q) + y_t(M:end); % actual prediction
        end
   end    % end loop over q
% ========================================================================= %
%~~~~~~~~~~~~~~~~~~~~~~~~~~~~~~~~~~~~~~~~~~~~~~~~~~~~~~~~~~~~~~~~~~~~~~~~~~%




% ~~~~~~~~Filter using just Static input signals~~~~~~~~~~~~~~~~~~~~~%
     % Seperate input and output
        [Nt P] = size(sys_dat{ss});
        N = 2*floor(floor(Nt/2)/2); %split data set in half. N must be even
        X = sys_dat{ss}(1:N,6:8);
        Y = sys_dat{ss}(end-N+1:end,1:Q);
% Initialize some Wiener Filter Parameters
[N,P]=size(X); [No,Q]=size(Y); W=zeros(M*P,Q); y_stat = zeros(No,Q);
% =============Start computing autocorrelation matrices================ %
    RX = xcorr(X,N/2,'unbiased'); R_X = {}; % compute correlation functions
    for i=1:P^2 % stack correlation functions into block Toeplitz corr.
matrices
          j= 1+floor((i-.2)/P);
```

```
          k =1+ mod(i-1,P) ;
         R_X{j,k} = toeplitz(RX(N/2+1:N/2+M,i));
    end
    R_X = cell2mat(R_X); % convert into big matrix.
          % figure(7); imagesc(R_X); colorbar;
    for q=1:Q % loop over output dimensions
        R_iy = zeros(P,M);
        for i=1:P % loop over input dimensions
            [c_iy, lags] = xcorr(X(1:No,i),Y(:,q),No/2,'unbiased') ;
            R_iy(i,:) = flipud(c_iy(No/2+2:No/2+M+1));
        end
            r_iy = reshape(R_iy',P*M,1)'; % cross correlation fxn
            W(:,q) =  (r_iy/R_X)';  % compute Weiner Filter Coefficients
        for i=1:P % loop over input dimensions
            y_t = conv(X(1:No,i),W(1+(i-1)*M:i*M,q));
            y_stat(:,q) = y_stat(:,q) + y_t(M:end); % actual prediction
        end
   end    % end loop over q
% ========================================================================== %
%~~~~~~~~~~~~~~~~~~~~~~~~~~~~~~~~~~~~~~~~~~~~~~~~~~~~~~~~~~~~~~~~~~~~~~~~~~~~%



% ~~~~~~~~Filter using just HUMAN input signals~~~~~~~~~~~~~~~~~~~~~%
     % Seperate input and output
        [Nt P] = size(sys_dat{ss});
        N = 2*floor(floor(Nt/2)/2); %split data set in half. N must be even
        X = sys_dat{ss}(1:N,[6,8]);
        Y = sys_dat{ss}(end-N+1:end,1:Q);
% Initialize some Wiener Filter Parameters
[N,P]=size(X); [No,Q]=size(Y); W=zeros(M*P,Q); y_hum = zeros(No,Q);
% =============Start computing autocorrelation matrices================ %
    RX = xcorr(X,N/2,'unbiased'); R_X = {}; % compute correlation functions
    for i=1:P^2 % stack correlation functions into block Toeplitz corr.
matrices
          j= 1+floor((i-.2)/P);
          k =1+ mod(i-1,P) ;
         R_X{j,k} = toeplitz(RX(N/2+1:N/2+M,i));
    end
    R_X = cell2mat(R_X); % convert into big matrix.
          % figure(7); imagesc(R_X); colorbar;
    for q=1:Q % loop over output dimensions
        R_iy = zeros(P,M);
        for i=1:P % loop over input dimensions
            [c_iy, lags] = xcorr(X(1:No,i),Y(:,q),No/2,'unbiased') ;
            R_iy(i,:) = flipud(c_iy(No/2+2:No/2+M+1));
        end
            r_iy = reshape(R_iy',P*M,1)'; % cross correlation fxn
            W(:,q) =  (r_iy/R_X)';  % compute Weiner Filter Coefficients
        for i=1:P % loop over input dimensions
            y_t = conv(X(1:No,i),W(1+(i-1)*M:i*M,q));
            y_hum(:,q) = y_hum(:,q) + y_t(M:end); % actual prediction
        end
   end    % end loop over q
% ========================================================================== %
%~~~~~~~~~~~~~~~~~~~~~~~~~~~~~~~~~~~~~~~~~~~~~~~~~~~~~~~~~~~~~~~~~~~~~~~~~~~~%
```

```
% ~~~~~~~~Filter using just WATER input signals~~~~~~~~~~~~~~~~~~~~~%
     % Seperate input and output
        [Nt P] = size(sys_dat{ss});
        N = 2*floor(floor(Nt/2)/2); %split data set in half. N must be even
        X = sys_dat{ss}(1:N,7);
        Y = sys_dat{ss}(end-N+1:end,1:Q);
% Initialize some Wiener Filter Parameters
[N,P]=size(X); [No,Q]=size(Y); W=zeros(M*P,Q); y_h2o = zeros(No,Q);
% =============Start computing autocorrelation matrices================ %
    RX = xcorr(X,N/2,'unbiased'); R_X = {}; % compute correlation functions
    for i=1:P^2 % stack correlation functions into block Toeplitz corr.
matrices
          j= 1+floor((i-.2)/P);
          k =1+ mod(i-1,P) ;
         R_X{j,k} = toeplitz(RX(N/2+1:N/2+M,i));
    end
    R_X = cell2mat(R_X); % convert into big matrix.
          % figure(7); imagesc(R_X); colorbar;
    for q=1:Q % loop over output dimensions
        R_iy = zeros(P,M);
        for i=1:P % loop over input dimensions
            [c_iy, lags] = xcorr(X(1:No,i),Y(:,q),No/2,'unbiased') ;
            R_iy(i,:) = flipud(c_iy(No/2+2:No/2+M+1));
        end
            r_iy = reshape(R_iy',P*M,1)'; % cross correlation fxn
            W(:,q) =  (r_iy/R_X)';  % compute Weiner Filter Coefficients
        for i=1:P % loop over input dimensions
            y_t = conv(X(1:No,i),W(1+(i-1)*M:i*M,q));
            y_h2o(:,q) = y_h2o(:,q) + y_t(M:end); % actual prediction
        end
   end    % end loop over q
% ================================================================== %
%~~~~~~~~~~~~~~~~~~~~~~~~~~~~~~~~~~~~~~~~~~~~~~~~~~~~~~~~~~~~~~~~~~~~~~%
```

```
% ~~~~~~~~Filter using ALL input signals~~~~~~~~~~~~~~~~~~~~~%
     % Seperate input and output
        [Nt P] = size(sys_dat{ss});
        N = 2*floor(floor(Nt/2)/2); %split data set in half. N must be even
        X = sys_dat{ss}(1:N,:);
        Y = sys_dat{ss}(end-N+1:end,1:Q);
% Initialize some Wiener Filter Parameters
[N,P]=size(X); [No,Q]=size(Y); W=zeros(M*P,Q); y_all = zeros(No,Q);
% =============Start computing autocorrelation matrices================ %
    RX = xcorr(X,N/2,'unbiased'); R_X = {}; % compute correlation functions
    for i=1:P^2 % stack correlation functions into block Toeplitz corr.
matrices
          j= 1+floor((i-.2)/P);
```

```
          k =1+ mod(i-1,P) ;
         R_X{j,k} = toeplitz(RX(N/2+1:N/2+M,i));
    end
    R_X = cell2mat(R_X); % convert into big matrix.
          % figure(7); imagesc(R_X); colorbar;
    for q=1:Q % loop over output dimensions
        R_iy = zeros(P,M);
        for i=1:P % loop over input dimensions
            [c_iy, lags] = xcorr(X(1:No,i),Y(:,q),No/2,'unbiased') ;
            R_iy(i,:) = flipud(c_iy(No/2+2:No/2+M+1));
        end
            r_iy = reshape(R_iy',P*M,1)'; % cross correlation fxn
            W(:,q) =  (r_iy/R_X)';  % compute Weiner Filter Coefficients
        for i=1:P % loop over input dimensions
            y_t = conv(X(1:No,i),W(1+(i-1)*M:i*M,q));
            y_all(:,q) = y_all(:,q) + y_t(M:end); % actual prediction
        end
   end    % end loop over q
% ========================================================================= %
%~~~~~~~~~~~~~~~~~~~~~~~~~~~~~~~~~~~~~~~~~~~~~~~~~~~~~~~~~~~~~~~~~~~~~~~~~~~%
for i=1:P % record weights from concatinated signal processing
   ws(ss,i) = mean(mean(abs(W(1+(i-1)*M:i*M,:)),2));
end
 val(ss) = mean(mean((Y-y_all).^2)); % is it during a massive error?


      E_all = zeros(1,Q);
   E_mov = zeros(1,Q);
   E_com = zeros(1,Q);
   E_stat = zeros(1,Q);
   E_hum = zeros(1,Q);
   E_h2o = zeros(1,Q);
   E_ndvi = zeros(1,Q);
   E_rand = zeros(1,Q);

      E_all2 = zeros(1,Q);
   E_mov2 = zeros(1,Q);
   E_com2 = zeros(1,Q);
   E_stat2 = zeros(1,Q);
   E_hum2 = zeros(1,Q);
   E_h2o2 = zeros(1,Q);
   E_ndvi2 = zeros(1,Q);
   E_rand2 = zeros(1,Q);

   E_all3 = zeros(1,Q);
   E_mov3 = zeros(1,Q);
   E_com3 = zeros(1,Q);
   E_stat3 = zeros(1,Q);
   E_hum3 = zeros(1,Q);
   E_h2o3 = zeros(1,Q);
   E_ndvi3 = zeros(1,Q);
   E_rand3 = zeros(1,Q);
```

```
% values = {'latitude';'longitude';'dispersion';'orientation'};
    for q = 1:Q;
% %         figure(1);% clf;
% %          subplot(2,Q/2,q);
% %          plot(Y(:,q),'k-','Linewidth',3);
% %          plot(y_mov(:,q),'g-','LineWidth',.5);
% %          hold on;
% %          plot(y_com(:,q),'o-','LineWidth',.5);
% %          plot(y_stat(:,q),'b-','LineWidth',.5);
% %          plot(y_ndvi(:,q),'m-','LineWidth',.5);
% %          plot(y_hum(:,q),'y-','LineWidth',.5);
% %          plot(y_h2o(:,q),'c-','LineWidth',.5);
% %           plot(y_all(:,q),'r-','LineWidth',.5);
% %          plot(Y(:,q),'k-','LineWidth',.5);
% %          title([ 'E',num2str(E),'i',num2str(ss)]);
% %          ylim([-1 1]); ylabel(values{q}); xlabel('hours');
% %
legend('mov','stat','ndvi','hum','h2o','all','real','Location','Best');
       % legend('real','all','mov','stat','ndvi','Location','SouthEast');

   E_all(q) = mean( (Y(:,q)-y_all(:,q)).^2)./std(Y(:,q));
   E_mov(q) = mean( (Y(:,q)-y_mov(:,q)).^2)./std(Y(:,q));
   E_com(q) = mean( (Y(:,q)-y_com(:,q)).^2)./std(Y(:,q));
   E_stat(q) = mean( (Y(:,q)-y_stat(:,q)).^2)./std(Y(:,q));
   E_hum(q) = mean( (Y(:,q)-y_hum(:,q)).^2)./std(Y(:,q));
   E_h2o(q) = mean( (Y(:,q)-y_h2o(:,q)).^2)./std(Y(:,q));
   E_ndvi(q) = mean( (Y(:,q)-y_ndvi(:,q)).^2)./std(Y(:,q));
   E_rand(q) = mean( (Y(:,q)-y_rand(:,q)).^2)./std(Y(:,q));


   E_all2(q) = mean( (Y(:,q)-y_all(:,q)).^2);
   E_mov2(q) = mean( (Y(:,q)-y_mov(:,q)).^2);
   E_com2(q) = mean( (Y(:,q)-y_com(:,q)).^2);
   E_stat2(q) = mean( (Y(:,q)-y_stat(:,q)).^2);
   E_hum2(q) = mean( (Y(:,q)-y_hum(:,q)).^2);
   E_h2o2(q) = mean( (Y(:,q)-y_h2o(:,q)).^2);
   E_ndvi2(q) = mean( (Y(:,q)-y_ndvi(:,q)).^2);
   E_rand2(q) = mean( (Y(:,q)-y_rand(:,q)).^2);

   E_all3(q) = mean( (Y(:,q)-y_all(:,q)).^2)./var(Y(:,q));
   E_mov3(q) = mean( (Y(:,q)-y_mov(:,q)).^2)./var(Y(:,q));
   E_com3(q) = mean( (Y(:,q)-y_com(:,q)).^2)./var(Y(:,q));
   E_stat3(q) = mean( (Y(:,q)-y_stat(:,q)).^2)./var(Y(:,q));
   E_hum3(q) = mean( (Y(:,q)-y_hum(:,q)).^2)./var(Y(:,q));
   E_h2o3(q) = mean( (Y(:,q)-y_h2o(:,q)).^2)./var(Y(:,q));
   E_ndvi3(q) = mean( (Y(:,q)-y_ndvi(:,q)).^2)./var(Y(:,q));
   E_rand3(q) = mean( (Y(:,q)-y_rand(:,q)).^2)./var(Y(:,q));


    end
```

```
%  % Remove errors induced by numerical round-off tolerance
%     rce = 1; % cut-off to detect RCOND singular matrix errors
%
% E_all2(E_all3>rce) = NaN;
% E_mov2(E_all3>rce) = NaN;
% E_com2(E_all3>rce) = NaN;
% E_stat2(E_all3>rce) = NaN;
% E_hum2(E_all3>rce) = NaN;
% E_h2o2(E_all3>rce) = NaN;
% E_ndvi2(E_all3>rce) = NaN;
% E_rand2(E_all3>rce) = NaN;
%
%
% E_mov3(E_all3>rce) = NaN;
% E_com3(E_all3>rce) = NaN;
% E_stat3(E_all3>rce) = NaN;
% E_hum3(E_all3>rce) = NaN;
% E_h2o3(E_all3>rce) = NaN;
% E_ndvi3(E_all3>rce) = NaN;
% E_rand3(E_all3>rce) = NaN;
% E_all3(E_all3>rce) = NaN;   % this must come last or it will change the
rest.


% average errors across prediction values q
 e_all = nanmean(E_all); e_mov=nanmean(E_mov);  e_com = nanmean(E_com);
 e_ndvi = nanmean(E_ndvi); e_rand = nanmean(E_rand);
 e_stat = nanmean(E_stat); e_hum = nanmean(E_hum); e_h2o = nanmean(E_h2o);
  Err(ss,:) = [e_all, e_mov,e_com, e_ndvi, e_stat, e_hum, e_h2o,e_rand];

 e_all2 = nanmean(E_all2); e_mov2=nanmean(E_mov2);  e_com2 = nanmean(E_com2);
 e_ndvi2 = nanmean(E_ndvi2); e_rand2 = nanmean(E_rand2);
 e_stat2 = nanmean(E_stat2); e_hum2 = nanmean(E_hum2); e_h2o2 =
nanmean(E_h2o2);
  Err2(ss,:) = [e_all2, e_mov2,e_com2, e_ndvi2, e_stat2, e_hum2,
e_h2o2,e_rand2];

   e_all3 = nanmean(E_all3); e_mov3 = nanmean(E_mov3);  e_com3 =
nanmean(E_com3);
 e_ndvi3 = nanmean(E_ndvi3); e_rand3 = nanmean(E_rand3);
 e_stat3 = nanmean(E_stat3); e_hum3 = nanmean(E_hum3); e_h2o3 =
nanmean(E_h2o3);
  Err3(ss,:) = [e_all3, e_mov3,e_com3, e_ndvi3, e_stat3, e_hum3,
e_h2o3,e_rand3];


end % end loop over sectors

Err_data{E} = Err;
ErrT(E,:) = nanmean(Err);
ErrM(E,:) = nanmedian(Err);
ErrT2(E,:) = nanmean(Err2);
ErrM2(E,:) = nanmedian(Err2);
ErrT3(E,:) = nanmean(Err3);
```

```
ErrM3(E,:) = nanmedian(Err3);
 clear sys_dat;
 end % end loop over elephants

 median(Err3(Err3(:,1)<1))
 % save compsig_data2 ErrT ErrM ErrT2 ErrM2 ErrT3 ErrM3 Err_data;

 %%
 clear all;  load compsig_data2;



bar1 = Err_data(1:13); bar2 = cell2mat(bar1');

C1 = [[0,0,1];
      [0,1,0];
      [1,0,.5]];

for k=1:13
    Anna = bar1{k};
%     figure(3); clf; bar(Anna(:,[1,2,4,5])) ;  ylim([0,5]);
%     legend('all','mov','ndvi','static');

    iAnna = 1./Anna;
    figure(3); clf; bar(iAnna(:,[2,4,5]),'stack') ;
    legend('mov','ndvi','static');  colormap(C1);
    set(gcf,'color','w');
    set(gca,'FontSize',18);  xlim([0,55]);

    iAnna2 = iAnna(:,[2,4,5]);
    [T,v] = size(Anna);

    for i=1:T;
    iAnna2(i,:) = iAnna2(i,:)/sum(iAnna2(i,:));
    end

    figure(4); clf; bar(iAnna2,'stack') ;
    legend('mov','ndvi','static','Location','EastOutside');  colormap(C1);
    set(gcf,'color','w'); set(gca,'FontSize',18); ylim([0,1]); xlim([0,55]);

    pause(3);
end


dpts = length(ErrM);
C = [0,2,2,1,3,3,3];
colordef white; figure(1); set(gcf,'color','w');
xlabels = {'All factors','Past mov.','CoM
mov.','NDVI','Static','Human','Water'};
figure(1); clf;
boxplot(ErrM(:,1:7),'plotstyle','compact','labels',xlabels,'colorgroup',C,'co
lors','rgbm','labelorientation','inline');
ylim([0,.7]);
```

```
   figure(2); clf;
   xlabels = {'All factors','Past mov.','NDVI','Static Feat.','Null Model'};
set(gca,'Xtick',1:4,'XTickLabel',xlabels,'FontSize',15);
   h = boxplot([ErrM(:,[1,2,4,5])],'notch','on','labelorientation','inline');
   set(gca,'Xtick',1:4,'XTickLabel',xlabels,'FontSize',14);
 ylim([0,.5]); ylabel('Normalized MSE');

   hText = xticklabel_rotate90(1.35:5.35,xlabels,30,1);
   set(hText,'FontSize',12);
   set(hText,'VerticalAlignment','baseline');
   set(gcf,'color','w'); ylabel('normalized MSE','FontSize',12);
   set(gca,'fontsize',12);


Q1 = zeros(1,8); Q3 = zeros(1,8);
for i=1:8,
    vals = sort(ErrM(:,i));
    qpts = round(dpts/4);
    ind1 = find(vals>0,qpts,'first');
    ind3 = find(vals>0,qpts,'last');
    Q1(i) = vals(ind1(qpts));
    Q3(i) = vals(ind3(1));
end
```